Iranian Journal of Science and Technology, Transactions of Civil Engineering (2022) 46:1969–1995
https://doi.org/10.1007/s40996-021-00806-5

RESEARCH PAPER

Optimal Seismic Design of Asymmetrical-plan Steel Buildings with Composite Castellated Floor Systems

Ali Kaveh[1] · **Amir Fakoor**[1]

Received: 11 November 2021 / Accepted: 14 December 2021 / Published online: 7 January 2022

Abstract
A cost optimization methodology for the main constituents of multistory asymmetrical-plan steel buildings comprising of composite castellated floor systems and 3-D steel moment-resisting frames with considering their structural interaction is proposed in this paper. The seismic performance of asymmetrical-plan steel buildings is prone to stress concentration, torsion, and coupled lateral-torsional effects. It is possible that altering the mass distribution of the asymmetrical-plan buildings by increasing the cost of floor solutions results in fitter stiffness properties with a lower cost such that the total cost of the building is reduced. To examine, the validity of this proposition the optimization method performs in two phases. In the first phase, a fine-tuned vibrating particle system algorithm optimally designs individual composite castellated floor systems of asymmetrical-plan steel buildings and provides a required search space. In the second phase, the ant colony system (ACS) algorithm with AS_{rank} strategy explores the resulting search space to determine the optimal distribution of the floor solutions in the floor bays of the building, which in conjunction with its equivalent framing design, leads to the optimal resultant solution. An ant memory mechanism is incorporated into the formulation of the ACS algorithm to reduce the computational cost. A new graph-based procedure for mapping arbitrary structural topology into the MTSP network is introduced. The unifying of the two-phase functions of the method facilitates the controlling of the principal beam-girder vibrational mode of the floor systems. The solutions of two examples demonstrate that the programmed optimization method could efficiently optimize the floor systems and 3-D frames of asymmetrical steel buildings by examining their interaction. The distribution of least-cost floor solutions proved to be the optimal floor distribution. In many intermediate solutions, increasing the cost of the floor solutions results in a reduction in the total cost of the asymmetrical-plan steel buildings.

Keywords Cost optimization · Optimum seismic design · Asymmetrical-plan steel buildings · Composite castellated floor systems · Meta-heuristic algorithms · Ant colony system (ACS) · Fine-tuned vibrating particle system (FT-VPS)

1 Introduction

Optimization problems are classified into two main categories: problems with *discrete* and problems with *continuous* design variables. The coincidence of both discrete and continuous variables in practical problems is most likely to happen and is classified as *mixed problems*. For most real-world optimization problems, the design variables have discrete nature. Exploring optimal solutions when dealing with discrete variables is a hard problem (Arora et al. 1994).

Metaheuristics are high-level *computational intelligence* techniques that obtain near-global solutions for optimum design problems within an algorithmic framework. They are recognized as unified optimization solvers for both kinds of discrete and continuous problems. Although they could find near-global solutions for real size problems, their performance is debilitated by issues such as parameter tuning, slow rate of convergence, and the requisite for a considerable computational time due to execution of significant function evaluations (Siarry and Metaheuristics 2016).

In this paper, two of the robust metaheuristic algorithms have been utilized. The first metaheuristic is a fine-tuned version of the vibrating particle system (FT-VPS) algorithm. The FT-VPS enhances the performance of VPS (Kaveh and Ghazaan 2017) by escaping from local optima, an approach that applies to steel–concrete composite structures. The

✉ Ali Kaveh
alikaveh@iust.ac.ir

[1] School of Civil Engineering, Iran University of Science and Technology, P.O. Box, 16846-13114 Narmak, Tehran, Iran

second algorithm is inspired by the autocatalytic mechanism observed in ant colonies. A graph-based procedure for mapping arbitrary structural topology into the modified traveling salesman problem (MTSP) is introduced (Wilson 1998). After the formation of the MTSP graph that reflects the structural topology, the ant colony system (ACS) algorithm (Dorigo et al. 1999) incorporated with the AS_{rank} strategy (Bullnheimer et al. 1999) is adopted to solve the cost optimization problems.

The resultant mass of steel buildings is mainly influenced by the design of flooring systems and becomes more prominent in structures with *large spans* requirements. The attachment of composite castellated beams (CB) and composite deck slabs (DS) through the welded shear studs produce an ideal resource of flooring systems for structures with long-span requirements. Researchers have proved that optimizing the main parts of the composite castellated floor systems (i.e. DS and CB) separately and combining the least-cost solutions do not necessarily give rise to the *optimal resultant* floor system. Due to the structural interaction of the main constituents of the composite floor systems, the optimal resultant solution will be obtained when the optimization of composite CBs performed for *costlier* DSs except the cheapest one (Kaveh and Fakoor 2021; Kaveh and Ghafari 2016).

The same notion may be valid for the optimum design of *asymmetrical-plan steel buildings*. Asymmetrical-plan steel buildings have a higher tendency to suffer torsion and stress concentration, due to eccentricity between the center of mass and center of resistance. The equation of motion of asymmetrical steel buildings is a function of both mass distribution and stiffness properties that are coupled through the stiffness matrix resulting in a coupled lateral-torsional motion. It is possible that increasing the cost of floor systems decreases the distance between the centers of mass and rigidity, increasing the symmetry of the structure. Increasing the structural symmetry alleviates the torsional effect and stress concentrations due to the asymmetry of the structure. In other words, a specific mass distribution with higher cost may lead to an equivalent stiffness property with the lower cost such that the total cost of the building is reduced. Consequently, the optimality of these systems by optimizing the floor systems separately without considering the framing design would be at issue.

As the preliminary steps clarify the posed uncertainty, we have proposed an optimization methodology capable of distributing numerous distinct sets of design solutions to floor bays of asymmetrical-plan steel buildings and designing the corresponding 3-D frames for individual distribution. The optimization method is to compare the total cost of each set of floor distributions to determine the *optimal combination* of the main constituents of the asymmetrical-plan steel buildings' composite castellated floor systems and rigidly connected steel frames.

Actualizing such a proposal is an intricate task. Availability of a search space containing various feasible solutions with different costs for distinct floor bays of the asymmetrical steel buildings is a necessity. Therefore, the optimization method is directed to operate in two phases:

In the first phase, the FT-VPS optimizes distinct floor bays of the steel buildings that possess different dimensions and loading conditions (i.e. simply the state) simultaneously and not only for the least-cost DS but also for the set of up to 15 costlier DSs. In the next phase, the ACS algorithm with AS_{rank} strategy explores the resulting search space for finding the optimal distribution of the floor solutions whose equivalent framing design leads to the least-cost steel building. The design of framing members for the distributions of floor solutions is performed by the auto-selection property of SAP2000 in an integrated optimization framework.

On one hand, plenty of researches have been conducted in the field of optimal design of composite steel–concrete floor systems, but the majority of them have just considered either an individual composite beam or a single floor bay. In some, it is assumed that optimal solution would be repeated in all floor bays of the building, or the effects of adjacent bays are simulated by uniform loads. However, these assumptions do not hold in reality. On the other hand, the focus of many studies is the optimization of 3-D steel frames. In these papers, the optimization of the flooring systems has been neglected and invariant area loads are considered for the floor systems. Notably, the first mode of vibration of composite floor systems is a function of both interior beams and girders designs. As a result, a unified optimum design of composite floor systems and 3-D steel frames enables the control of the principal beam-girder mode of vibration.

Poitras et al. (2018) proposed a new trajectory metaheuristic algorithm entitled peloton dynamics optimization (PDO) that mathematically mirrors the mutual energy benefits of drafting that occurs during a bicycle race. The PDO algorithm performed consistently for three non-composite steel deck floor systems and proved to be better than particle swarm optimization (PSO) and harmony search (HS) algorithms. Kaveh and Ghafari (2018), in an optimization study of simply supported composite CBs, conclude that applying semi-rigid connections and non-commercial cutting shapes could reduce the cost by up to 25% and 35%, respectively. Kaveh and Shokohi (2015) implemented population-based meta-heuristic algorithms for optimum design of three simply supported non-composite perforated beams by the rules of the European standard. They considered both circular and hexagonal cutting shapes for optimization. The results demonstrate that castellated beams are more economical than cellular beams. They also optimized non-composite perforated beams by the natural forest regeneration (NFR) algorithm. The results prove that the NFR performs better than other metaheuristics considering both aspects of cost

minimization and convergence rate (Kaveh and Shokohi 2016).

Safari et al. (2021) optimally designed planar steel frames by a differential evolution (DE) based algorithm. The solution of the examples indicates that DE can perform as well as other metaheuristic algorithms. Hasansebi and Kazemzadeh Azad (2019) examined the performance of the adaptive dimensional search (ADS) algorithm, which uses an efficient performance-oriented methodology for discrete sizing optimization of spatial steel frames. The comparison of the algorithm with other metaheuristics demonstrates that the ADS algorithm could be efficiently employed for the optimization of real-size steel frames. Kaveh et al. (2017) optimized the weight of a 6-story regular 3-D steel moment-resisting frame by nine metaheuristic algorithms. The frame is analyzed under the combined effects of gravity and seismic loads distributed by modal response spectrum analysis (MRSA). They considered three expected levels of ductility for the frames, namely ordinary moment frame (OMF), intermediate moment frame (IMF), and special moment frame (OMF). For all levels of ductility, the HS algorithm was capable of minimizing the weight of the frame to a higher degree. Notably, the weight of the OMF is lower than the IMF and SMF by 2.9% and 7.1%, respectively. Hasancebi et al. (2010) compared the performance of seven metaheuristic algorithms in optimizing the weight of moment resisting spatial steel frames. The optimization algorithms are computerized in Borland Delphi and are automated to interact with SAP2000. Although metaheuristics are problem dependent, evolution strategies and simulated annealing algorithms proved to be the most effective methods, considering both aspects of weight minimization and convergence rate.

For fulfilling the aim of this study, efficient optimization algorithms with reasonable computational costs must be applied. Regarding this empirical subject, the theory is not considerable guidance. As the solver of the mixed optimization problem of the first phase, the FT-VPS algorithm that specifically targets the optimization of composite steel–concrete floor systems and enhances the performance of its inceptive version (VPS) proved to be a suitable algorithm.

Kaveh and Ghazaan (2017) proved the superiority of the VPS algorithm in comparison to the other metaheuristics for optimization of truss and planar steel frame structures. The results of numerous independent runs performed using the benchmark examples indicate the reliability and efficiency of the VPS algorithm for solving the constrained optimization problems of skeletal structures. Kaveh and Fakoor (2021) proved the superiority of the VPS algorithm for practical optimization of an individual composite castellated floor system with perimeter composite castellated beams compared to other non-deterministic optimization methods. To improve the performance of the VPS algorithm and secure more reliable solutions, we have conceived fine-tuning mechanism to escape from local optima. The convergence plots of the first phase of the test examples that are depicted after the onset of the fine-tuning mechanism prove the efficiency of the implemented approach.

The problem of cost optimization of asymmetrical-plan steel buildings with composite castellated floor systems has not been solved by existing metaheuristic algorithms before. By considering the nature of the design variables, cost, and constraint functions the well-known ACS algorithm with AS_{rank} strategy that could directly manipulate the discrete variables is adopted as the solver for the combinatorial optimization problem of the second phase. Although it is difficult to tune ant-based algorithms, we have succeeded in setting the most suitable algorithm parameters.

The performance of ant-based optimization techniques is proved to be better than evolutionary methods. Although both ACO and GAs are population-based metaheuristics, it is only ACO that stores the information in pheromones that represent the collective memory of all individuals of the colony from all generations. Despite the GAs, ACO refrain from an unproductive search in less promising regions due to poor initial solutions via combining learned information explored by the entire colony and the initial value of pheromone trails (Camp et al. 2005). Camp et al. (2005) utilized the ACO algorithm for size optimization of planar steel frames. They proved that the ACO, in comparison to genetic algorithms (GA), is capable of obtaining lighter solutions by up to 14% in fewer frame analyses. Aydogdu and Saka (2012) optimized symmetrical-plan and asymmetrical-plan 3-D steel frames by ACO algorithm for studying the effect of wrapping on the optimal solutions. The results reveal that the ACO algorithm could efficiently optimize the spatial steel frames. It could be observed that the inclusion of the wrapping effects increases the weight of both symmetrical-plan and unsymmetrical-plan steel frames by 9% and 12%, respectively.

Some recent advancements in the practical application of metaheuristic algorithms in the optimal design of structural engineering problems are reviewed in the upcoming literature. In computationally expensive optimization problems in which only a few runs are affordable, the small number of independent runs becomes highly valuable. Kazemzadeh Azad (2019, 2021) developed a solution for exploiting the available computing power entitled monitoring convergence curve (MMC) for dealing with such problems. The MMC monitors the convergence curve of the succeeding runs of the implemented algorithm at certain intervals based on the information of the previous run. The test examples reveal the effectiveness of the MMC considering both aspects of quality and stability of the optimal solutions of truss and frame structures. Hasansebi et al. (2011) effectively optimized the member size of high-rise steel buildings utilizing evolution strategy integrated parallel algorithm. They

defined an index in the form of (a × b) for measuring the effect of computational cluster size on the execution time of the algorithm where (a) stands for the number of processors in each computer and (b) for the number of computers. The results reveal that the maximum parallel processing speed up ratio between 12.2 and 16.8 is obtained by utilizing a cluster size with the index of (4 × 8). Kazemzadeh Azad et al. (2013, 2014) proposed an upper bound strategy (UBS) for decreasing the number of structural analyses for computationally expensive structural optimization problems. The UBS prevents the fitness calculation of newly generated solutions unless their net cost does not exceed the fitness of the interim optimum solution. The results indicate that UBS is capable to decrease the number of structural analyses up to 97.1% and 70% in medium and large-scale 3-D steel frames, respectively. Kaveh and Ghazaan (2018) optimized the weight of irregular spatial steel frames by CBO, ECBO, VPS, and a hybrid algorithm based on VPS (MDVC-UVPS). The results reveal that the MDVC-UVPS and VPS ranked first and second in performance assessment of the algorithms, respectively. Implementation of the UBS in the initial iteration of the optimization process with a high amount of infeasibilities of the candidate solutions is less efficient. Kazemzadeh Azad (2018) prescribed a non-algorithmic procedure that is seeding the initial population with feasible solutions for overcoming this deficiency. The proposed procedure seeds the initial population by the largest cross-section and an intermediate section which leads to the lightest feasible design in the discrete design pool.

As the building becomes more asymmetrical the detrimental effects of torsion and stress concentration will increase. In addition, the seismic performance of asymmetrical-plan steel buildings is influenced by the coupled lateral-torsional effects. Hence, if a search space containing multiple design solutions with various costs for distinct floor bays of a steel building were accessible, the optimality of the least-cost heuristics (i.e. distribution of least-cost solutions to all the floor bays) and determination of stiffness properties to such *mass distribution* would be questionable. The proposed method examines the validity of such a proposition for rigidly connected steel buildings with composite castellated floor systems.

Firstly, the optimization method generates the prerequisite search space throughout the first phase of its operation. Next, it becomes capable to determine the optimal distribution of design solutions to the floor bays of the building in a way that their equivalent framing design gives rise to the least-cost resultant steel building.

In the first phase, the optimization method simultaneously optimizes individual floor bays of the building which possess distinct states. In addition to determining optimal design variables that directly lead to a reduction in material costs (i.e. root beam of CBs), the method applies supplementary structural techniques for further reduction in the final cost of each floor state. Besides considering costlier DSs, these techniques comprise optimizing the *shape parameters* of hexagonal perforations and defining the optimal number of *floor divisions* (i.e. interior beams). Inclusion of partial composite action, infilling certain openings, and specifying camber are supplementary techniques that prevent an increase in the cost of composite CBs (Kaveh and Fakoor 2021).

Bearing in mind that the design of low-cost systems without compromising the integrity of the structure is an essential issue in an optimal design process, a robust design procedure forms the set of 28 constraints of the composite CBs optimization problems (Kaveh and Fakoor 2021). Both the optimization and design procedures of composite castellated floor systems are coded in MATLAB.

In the second phase, the ACS algorithm with AS_{rank} strategy explores the resulting search space to determine the optimal distribution of design solutions for the floor bays of the building, such that corresponding proportions of framing members lead to an optimal resultant structure. The optimization process of this phase is compiled in MATLAB (MATLAB, Version 9.7 R2019b, The MathWorks, Inc., Natick, Massachusetts, United States) and is automated to interact with SAP2000 (CSI SAP2000 Integrated Software for Structural Analysis and Design, Version 19.2.0, Computers and Structures Inc., Berkeley, California) that performs gravitational and seismic design of the steel frames in an integrated practice. The seismic design is performed according to the MRSA procedure. In addition to the strength and deflection constraints imposed on each set of candidate framing members by SAP2000, the optimization method facilitates the controlling of vibrational constraints for the supporting girders of composite castellated floor systems.

All things considered, a comprehensive cost optimization methodology comprising of three modules for main constituents of asymmetrical-plan steel buildings including composite deck slabs, composite castellated interior beams, and spatial moment-resisting steel frames without excluding their structural interactions is proposed in this research.

This paper is divided into 6 sections: In Sect. 2, the principles and features of the proposed optimization method are elaborated on. Section 3 formulates the mathematical statements of the optimal design problems. In Sect. 4, the implemented optimization algorithms are presented. In Sect. 5, the performance of methodology is verified by implementing two design examples, and finally, Sect. 6 concludes the paper.

2 Definitions and Concepts

2.1 Deck Slab Optimization Module

The proposed optimization method has been enabled to work with two of Canam (2006) composite deck profiles namely P-3623 and P-2432. Each deck profile is fabricated by the combination of three invariant deck thicknesses (t_d) and six slab depths (t_s) providing a set of 18 DS sections. In the first iteration of the design procedure, one interior beam is considered for candidate DS which divides the bay into two parts. Then, the constraint check and cost calculation are performed based on the resulting span (B). The cost function is adjusted to be a function of a number of floor divisions (n_{fd}). Thus in the next iteration, one interior beam is added and the parametric optimization is repeated for the resulting new span. This process is repeated for the available deck slab sections. Ultimately, feasible DSs will be sorted based on their cost in ascending order. The lightweight concrete and shored spans are disregarded in the current work. The deck slab optimization module is applied for distinct floor bays of unsymmetrical-plan steel buildings.

2.2 Composite Castellated Beam Optimization Module

To improve the performance of the VPS algorithm and secure more reliable solutions, we have conceived '*fine-tuning mechanism*' to escape from local optima. The performance of the fine-tuning mechanism is such that after the optimization of CBs for the first n_r feasible DSs, the solutions are collected based on the number of floor divisions. For each collection, the solution of the interior beams with the least cost is identified and substituted for all the members of the group. The objective function of the new solutions is then reobtained and if they prove to be fitter than their previous record, replacements occur.

FT-VPS selects the design variables of composite CBs intelligently in such a way that the *manufacturing cost* turns out to be minimized. While this is the main concern of the majority of articles, the proposed method also examines several procedures for further reduction of the total cost of the composite castellated floor systems. If the assumption of full composite action is violated, the optimization method is enabled to design *partially composite CBs*. This process could prevent the rise of the additional steel cost. The *infilling holes' technique* works in a way that if any of the tee sections or the web posts violate the beam–column interaction equation, the corresponding hole would be covered by a single plate with the same thickness as the posts. If the number of filled holes exceeds half of the total number of holes a penalty would be imposed for the candidate beam. This technique recompenses the constraint violation without additional penalty up to half of the perforations. The *camber specifying mechanism* works in a way that if a composite CB violates any of the total deflection constraints, before foisting additional penalty a camber equal to the value of the self-weight deflection would be specified. Afterward, the assessment of violated criteria would be repeated.

The optimization procedure of composite CBs is performed for a certain number of costlier deck slabs. The composite CB optimization module is applied for all the floor bays of the buildings which possess individual geometry and loading condition (i.e. state).

2.3 Steel Building Optimization Module

In this phase, each of the floor bays of the asymmetrical-plan buildings, regardless of their states, could be specified as an individual design variable. Nevertheless, it is still their state that defines their equivalent search space. Taking constructional considerations into account, it is possible to consider an arbitrary number of floor bays with a similar state, as the same design variable. Although the utilization of CBs makes the construction of longer spans possible without increasing the weight of the structures, the reentrant corners of their hexagonal holes are bases for stress concentration ergo limiting their use in environments with high levels of seismic excitations (Fares et al. 2016). Consequently, CBs are not considered as seismic load-bearing members and the plain webbed beams have been utilized as the horizontal seismic members of 3-D framing assembly in the current study.

The ACS algorithm with AS_{rank} strategy searches for the *optimal mass distribution* of the MDF dynamic system that together with its equivalent stiffness properties results in the optimal design solution. The focus of the current study is limited to the internal forces of beams and columns, beams deflections, and girders vibration of the spatial steel frames. Structural evaluation and fitness calculation is one of the steps of the optimization process with the ACS algorithm (Table 2). In this step, the *primary program* (MATLAB) is incorporated with a novel attribute associated with the integrated optimization procedure that is fully automated to interact with SAP2000 (i.e. *replica*). The primary program calculates the applied loads to the beam members of the frames corresponding to each set of the candidate solution of the floor systems and transfers the loads to the replica. Earthquake loads are calculated based on the MRSA procedure by the replica. Afterward, the replica automatically assigns the most economical previously defined section lists to the frame objects. After the completion of the analysis and

design procedure of framing members, the replica delivers the number of failed elements to the primary program.

At this step, the primary program could evaluate arbitrary constraints whose evaluation could not be performed directly by the replica. In the current study, the primary program facilitates the examination of the *vibrational constraints* of floor bays based on the principal combinatory beam-girder mode. The main program calls for the geometric properties and nodal displacements of the girders from the replica and calculates their deflections at the points where the interior beams are connected. It also calculates maximum deflections of the connected interior composite CBs based on the Benitez method (1998). The required data is obtained and the natural frequencies and required damping ratios based on Murrie's method (1991) are calculated respectively. The vibrational constraints are to be evaluated for the supporting girders and the number of failed elements updated subsequently. Afterward, the primary program calls for the surface area of the framing members to calculate the total weight of the 3-D frames. At the last stage, the primary program calculates the fitness of the candidate steel building. The 'primary/replica interaction' of the optimization framework in the second phase is illustrated in Table 1.

It is known that the overall computational time of structural evaluations consumes 85–95% of the total computing time of an optimal design process. In order not to squander time, an "ant memory mechanism" is incorporated into the formulation of ACS algorithm that saves unique solutions explored by the ants. At the beginning of each iteration, the refurbished positions are checked in the ant memory matrix, to avoid repetition. Incorporating such a mechanism prevents a repetition of structural evaluations and, hence saving a considerable amount of computational cost. The ant memory matrix also provides a range of feasible floor distributions with various costs, which could be utilized considering the constructional considerations.

The load path in steel building determines the unidirectional sequence of the practical optimization process. The load path and the resulting sequence of the optimization process are illustrated in Fig. 1.

For *decoupling* the main constitutes of steel buildings, namely composite castellated floor systems and moment-resisting steel frames, firstly the optimization of distinct floor systems of the building is performed. In the next step, the ant colony in each iteration of the ACS algorithm distributes the specific discrete variables of the floor solutions in the floor bays of the steel building. The floor distribution explored by each ant converts to the equivalent concentrated and uniform loading. The corresponding loads are applied to individual girders and edge beams of the spatial steel frame according to the general procedure depicted in Fig. 2.

3 Problem formulation

For the most complex structural systems, the entire design project must be broken down into several subproblems which are then treated independently. Each subproblem can be posed as a problem of optimization. The number of sub-optimization problems are obtained by the following expression as $1 + \sum_{i=1}^{n} (n_r^i + 1)$, where n denotes the number

Table 1 Primary/replica interactive performance

Primary assignments (MATLAB)			Replica assignments (SAP2000)
Load erasing command	→		Erasing previous loads
Calculation of loads of frame beams			Hold
Sending loads of the frame beams	→		Applying loads to frame members
Analysis command	→		Perform analysis
Design command	→		Perform design
Call for the number of failed elements	→	←	Sending the number of failed elements
Call for the girders sectional properties	→	←	Sending the girder sectional properties
Call for the girder nodal displacement	→	←	Sending the girder nodal displacements
Evaluation of the vibrational constraints			Hold
Updating the number of failed elements			Hold
Call for the sectional properties of frame elements	→	←	Sending the sectional properties of frame elements
Calculation of the total frame weight			Hold
Calculation of the fitness of steel building			Hold

of floor states and $n_r^i \leq 15$ is the number of feasible DSs for each state. The renowned three stages of mathematical formulation for sub-optimization problems are outlined in detail in the following literature. It must be noted that the problem formulation of the DSs and CBs is written for one of the floor states which is also applicable to other states.

3.1 Formulation for Deck Slab Design

The program is able to utilize the DSs provided by the Canam (2006) composite P-3623 and P-2432 profiles. Therefore, variables that characterize an individual profile shape (i.e. h_r, w_r and d_r) are all merged into a single discrete variable (P-No.). The other two discrete variables are steel decks' thickness (t_d) and total slab thickness (t_s) and are illustrated graphically in Fig. 3. Another discrete variable is the number of floor divisions (n_{fd}). Consequently, the design variables are given as:

$$x_{DS}^i = (\text{P - No.}, t_d, t_s, n_{fd}) \qquad \text{i} = 1 \text{ to } n_r^i \leq 15 \tag{1}$$

The extended cost function of the DS subproblems that takes into account both fabrication and material costs of all constituents of the floor system is written as:

$$C_{DS}^i = C_{\text{material}}^i + C_{\text{fabrication}}^i \tag{2}$$

The material cost of composite DSs depends on the weight of steel elements and the volume of the concrete elements as follows:

$$C_{\text{material}}^i = W_d^i k_d + V_c^i k_c, \tag{3}$$

where $\text{W}_d^i = \text{A}_{\text{bay}} \text{w}_d^i$ is the weight of the steel decks;$\text{V}_c^i = \text{A}_{\text{bay}}(\text{w}_c^i / \gamma_{\text{c}})$ is the concrete volume; k_d and k_c are the cost factors for steel decks and concrete slab; $w^i{}_d$ and $w^i{}_c$ are the steel deck and concrete weights per unit area. On-site fabrication cost of the composite DSs is related to the area of the constructional operation as:

$$C_{\text{fabrication}}^i = A_f k_f \tag{4}$$

A_f is the surface area of the bay and k_f is the fabrication cost factor of the DS. The feasibility of the DSs is verified by the following constraints:

$$\overline{g}_1^i = W_f - W_r \leq 0 \tag{5}$$

$$\overline{g}_2^i = \Delta_L - \Delta_{al} \leq 0 \tag{6}$$

$$\overline{g}_{3,4}^i : \quad B_{\min} \leq B \leq B_{\max} \tag{7}$$

$$\overline{g}_5^i : \quad B - B_{MUS-3} \leq 0. \tag{8}$$

3.2 Formulation for Composite Castellated Beam Design

Clear depth of the web, web thickness, flange width, flange thickness, and root radius are the main parameters that define the sectional parameters of I-shaped members. Parameters that characterize the root beam section of CBs are merged into a single discrete variable denoted by B_j. The design variables that define the shape of hexagonal perforation of CBs are the height of the holes or posts from the center (h), the minimum width of the holes or posts (e), and the angle of inclination (θ) of the openings. These variables are sketched in Fig. 4. Thus, the set of design variables for optimum design of CBs is written as:

$$x^i = (B_j, h, e, \theta); \quad i = 1 \text{ to } n_r \leq 15 \tag{9}$$

The extended cost function of CB subproblems takes the following form:

$$C_{CB}^i = C_{\text{material}}^i + C_{\text{fabrication}}^i \tag{10}$$

Material cost of CBs depends on the weight of steel elements as:

$$C_{\text{material}}^i = \sum_{j=1}^{3} W_j^i k_j, \tag{11}$$

where $j = 1$–3 corresponds to steel components of CBs including the root beams, fillers, and the shear studs, respectively; $W_1^i = LG_1^i$ and $W_{2,3}^i = \gamma_s \ V_{2,3}^i$ are the weight of steel components; G is the weight of the root beams per unit length; $V_{2,3}$ are the volume of fillers and shear studs, respectively; γ_s is the steel density; and k_j is the cost factor of steel components. The fabrication cost of CBs is related to the length of the manufacturing operations as:

$$C_{\text{fabrication}}^i = \sum_{m=1}^{3} L_m^i k_m, \tag{12}$$

where $m = 1,2$ and 3 represent the individual operation of the fabrication process consisting of cutting, welding, and cambering, respectively. L_1^i is the cutting length; L_2^i is the welding length and $L_3^i = I_o^{-1}(I_{cn}\delta_c)^i$ is the normalized length of cambering; I_o is the minimum strong axis moment of inertia in the section pool; I_{cn} is the transformed moment of inertia of composite net section. k_m is the cost factor of each fabrication operation.

The constraints that govern the optimization problem of composite CBs fall into 3 categories; the first type represents

the limitation of the sectional shape parameters. The second and third types correspond to strength and deflection limit states, respectively.

3.2.1 Type 1

The manufacturing and geometrical constraints of CBs are as follows (Kaveh and Shokohi 2016):

$$h_1^i = h - (3/8)(d_g - 2t_f) \le 0 \tag{13}$$

$$h_2^i = (d_g - 2t_f) - 10(d_t - t_f) \le 0 \tag{14}$$

$$h_3^i = (2/3)b - e \le 0 \tag{15}$$

$$h_4^i = e - 2b \le 0 \tag{16}$$

$$h_5^i = 2b + e - 2h \le 0 \tag{17}$$

$$h_{6,7}^i : \quad 43 \le \theta \le 62 \tag{18}$$

$$h_{8,9}^i : \quad 10 \le \xi \le 30 \tag{19}$$

$$h_{10}^i : \quad \eta \le 8. \tag{20}$$

3.2.2 Type 2

In comparison to plain webbed beams, many additional failure modes govern the design of composite CBs as a result of several web openings. The limit states that govern the strength design of composite CBs are local buckling of tee components; flexural buckling of top tees and web posts; tensile yielding of bottom tees; the plastic moment of tees; LTB of tees; interaction criteria of tees and posts; shear yielding and shear buckling of tees, gross section and posts; web post lateral instability (Fares et al. 2016; Blodgett 1966). The corresponding constraints are formulized in adherence with LRFD principles of the 2016 version of AISC Specification (ANSI 2016). The existing design theory is completed by the authors via the inclusion of the interaction criterion for web posts subjected to combined compression and flexure (Kaveh and Fakoor 2021). When the CBs are subjected to wall loads, concentrated loads, and dynamic forces, implementation of the proposed design method is highly recommended.

$$g_1^i = \lambda_{\text{f - top - tee}} - 0.56\lambda_0 \le 0 \tag{21}$$

$$g_2^i = \lambda_{\text{s - top - tee}} - 0.75\lambda_0 \le 0 \tag{22}$$

$$g_3^i = \lambda_{f-tees} - 0.38\lambda_0 \le 0 \tag{23}$$

$$g_4^i = \lambda_{s-tees} - 0.84\lambda_0 \le 0 \tag{24}$$

$$g_5^i = T_{\text{u - bottom tee}} - T_{\text{c - bottom tee}} \le 0 \tag{25}$$

$$g_6^i = P_{\text{u - top tee}} - P_{\text{c - top tee}} \le 0 \tag{26}$$

$$g_7^i = M_{\text{u - tees}} - M_{\text{c - tees}} \le 0 \tag{27}$$

$$g_8^i = N_{\text{fh(i)}} - 0.5N_{\text{h}} \le 0 \tag{28}$$

$$g_9^i = P_{u-post} - P_{c-post} \le 0 \tag{29}$$

$$g_{10}^i = M_{\text{u - post}} - M_{\text{c - post}} \le 0 \tag{30}$$

$$g_{11}^i = N_{\text{fh(j)}} - 0.5N_{\text{h}} \le 0 \tag{31}$$

$$g_{12}^i = V_{u-ver-tees} - V_{c-ver-tees} \le 0 \tag{32}$$

$$g_{13}^i = V_{u-ver-gross} - V_{c-ver-gross} \le 0 \tag{33}$$

$$g_{14}^i = V_{u-hor-post} - V_{c-hor-post} \le 0. \tag{34}$$

3.2.3 Type 3

The web opening of CBs reduces the gross moment of inertia that increases the curvature at web openings, causes the incompatibility of strain field, and reduces the gross area between tees results in the formation of Vierendeel deflections. For each stage of construction, pre and post concrete hardening, different approaches with utmost accuracy are adopted for estimating the maximum deflection of CBs (Fares et al. 2016; Benitez et al. 1998).

$$s_1^i = \delta_{L1} - \delta_{al} \le 0 \tag{35}$$

$$s_2^i = \delta_{T1} - \delta_{at} \le 0 \tag{36}$$

$$s_3^i = \delta_{L2} - \delta_{al} \le 0 \tag{37}$$

$$s_4^i = \delta_{T2} - \delta_{at} \le 0 \tag{38}$$

Detail description of the equations for all types of constraints can be found in Kaveh and Fakoor (2021). The

penalization approach is implemented for constraint handling. Thus, the evaluation function which is the penalized cost function of the problem is calculated as:

$$eval^i_{CB} = n^i_b \, P^i \, C^i_{CB} \tag{39}$$

$$P^i_{\text{CB or Frames}} = \begin{cases} 1 \;\; if\, x \in \mathbb{F} \\ (1+\varepsilon_1 v^i)^{\varepsilon_2} \;\; \text{otherwise,} \end{cases} \tag{40}$$

where $n_b{}^i = n_{fd}{}^i - 1$ is the number of interior beams. P^i_{CB} is the dynamic penalty function; $v^i = \sum_{n_{CB}=1}^{28} \max\left[0, g^i_n(x)\right]$ represents the sum of the violations of the constraints. n_{CB} is the numerator of the constraints applied to interior CBs; Here, ε_1 is set to unity and $\varepsilon_2 = 1.5\,(1 + I_t/I_m)$,where I_t is the current iteration number and I_m is the maximum number of iterations.

Consequently, a complete set of design variables that describe the optimization of composite castellated floor systems excluding the vibrational constraints becomes:

$$x^i_{Floor} = (\text{P - No.}, t_d, t_s, n_{fd}, B_j, h, e, \theta) \tag{41}$$

And, the total cost of composite castellated floor systems is obtained as:

$$C^i_{Floor} = C^i_{DS} + eval^i_{CB} \tag{42}$$

3.3 Formulation for Steel Building Design

Design variables are divided into two types. In the first type, each solution for the floor bays is represented by a discrete variable that is the main design variable of the optimization problem. The second type is discrete variables of the frame members that are the subordinate variables of the problem.

$$x_{\text{Steel Building}} = (\text{Floor}_{\text{ij}}, \text{Section}_{\text{rs}}) \text{ where } \begin{cases} 1 \le i \le n_v \\ 1 \le j \le n^i_r \end{cases}; \quad \begin{matrix} 1 \le r \le n_m \\ 1 \le s \le n_s, \end{matrix} \tag{43}$$

where i is the numerator of the variable of the floor bays whose upper bound is the total number of flooring variable (n_v); j is the index number of the floor solution whose upper bound is the equivalent size of the search space ($n^i_r \le 15$). r is the numerator of the framing members whose upper bound is the total number of members of the 3-D frames (n_m). s is the index number of the framing sections and its upper bound is the size of the section pool (n_s). The cost function of the steel building problem is written as:

$$\begin{aligned} C_{\text{Steel Building}} &= C_{\text{Floors}} + eval_{\text{Frames}} \\ &= \sum_{i=1}^{n_v} n_i C_{ij} + P_{\text{Frames}} C_{\text{Frames}}, \end{aligned} \tag{44}$$

where n_i is the number of floor bays in the building which are classified as the of i^{th} flooring design variable; C_{ij} is the total cost of j^{th} solution assigned to i^{th} variable; P_{frames} is the penalty function of spatial frames which is calculated as stated previously by considering $v = n_{fm}/n_m$,where n_{fm} is the total number of failed members of the frames; $\varepsilon_1 = 10$ and ε_2 is calculated as before.

$$\begin{aligned} C_{frames} &= W_{frames}\, k_s \\ &= \left(\sum_{m=1}^{n_m} \gamma_s L_m A_m \right) \times k_s \end{aligned} \tag{45}$$

W_{frames} is the total weight of the steel frames, L_m and A_m are the length and surface area of the m^{th} member of the steel frames.

SAP2000 controls the girders and edge beams of 3-D frames for bending moment, shear, and deflection constraints. It also controls axial force, bending moments, the interaction of the axial force and bending moments, and shear constraints for the column members. The constraints that are directly controlled by SAP2000 are classified as Type 4 constraints. The mathematical relations of these constraints are omitted for brevity.

Annoying floor motion induced by building occupants is probably the most persistent floor serviceability problem encountered by designers. The composite castellated floor systems are complex and have multiple natural frequencies. Murray's acceptability criterion is the most widespread use by structural designers for the evaluation of the first natural frequency (Murray 1991; Naeim 1991). Combinatory beam-girder vibrational constraints are applied by the interactive primary/replica mechanism for each of the frame girders and its connecting interior beams, concerning the position of the girder. Based on its position, each girder is adjacent to either one or two floor bays. Thus, $G \le G_1 + 2G_2$ is the numerator of girders where G_1 are the girders adjacent to a single bay and G_2 are the girders adjacent to two bays. The relations regarding the beam-girder vibrational constraints that are categorized as Type 5 are written as:

3.3.1 Type 5

$$s^G_1 = 8 - \zeta_e \le 0 \tag{46}$$

$$s^G_2 = 10 - f_n \le 0 \tag{47}$$

$$s^G_3 = \zeta_{req} - \zeta_c \le 0 \tag{48}$$

The type 5 constraints are elaborated in Naeim (1991).

4 Optimization methods

The VPS formulation reflects a basic *structural engineering* notion that is the free vibration of ideal one-story frame structures with viscous damping (Kaveh and Fakoor 2021). VPS regeneration equation embodies the fundamentals of metaheuristic optimization techniques consisting of self-adaptation, cooperation, and competition. The formulation of the FT-VPS algorithm for cost optimization of the composite castellated beams is described in the upcoming section (Kaveh and Ghazaan 2017).

4.1 Formulation of FT-VPS algorithm

Step 1 Initialization phase

The vibrating frame matrices (VFs) which contain the initial positions of ideal frames are initialized as:

$$x^{i}_{initial(j)} = x^{i}_{\min(j)} + rand.\left(x^{i}_{\max(j)} - x^{i}_{\min(j)}\right), \tag{49}$$

where $x^{i}_{\text{initial (j)}}$ is the initial position of the jth variable of the ith ideal frame, $x^{i}_{\min(j)}$ and $x^{i}_{\max(j)}$ are its side limits and rand is random numbers drawn from the standard uniform distribution on the closed interval [0,1].

Step 2 Evaluation of candidate frames

In the next step, the cost matrix (CM) which contains the fitness of the ideal frames is evaluated. During the evolutionary process, the algorithm examines the fitness of the population and if any improvement is detected, the new cost and its equivalent position are substituted in RM and VFM matrices, respectively.

Step 3 Search phase

FT-VPS improves the position of ideal frames by simulating the damped free vibration by the following equation:

$$\begin{aligned} F_{new(i)} = {} & \omega_1\left(A.D.rand + F_o\right) + \omega_2\left(A.D.rand + F_{S(i)}\right) \\ & + \omega_3\left(A.D.rand + F_{I(i)}\right) \end{aligned} \tag{50}$$

Parameter A is introduced to model the amplitude of free-vibration response as:

$$A = \omega_1(F_o - F_i) + \omega_2(F_{S(i)} - F_i) + \omega_3(F_{I(i)} - F_i) \tag{51}$$

And damping ratio is simulated by the following relation:

$$D = \left(\frac{I_t}{I_m}\right)^{-c}, \tag{52}$$

where F_o is the interim optimum frame that is the optimum solution of the population so far; F_s and F_I are the superior and inferior frames, respectively. To determine the intermediate frames at each iteration, CM is sorted in ascending order and F_S and F_I are selected randomly from the first and second halves, respectively, except the frame itself. ω_i are the weight coefficients.

The following stochastic relations increase the rate of convergence which must be checked before applying the regeneration formula:

$$\begin{cases} If\ pro < rand \Rightarrow w_3 = 0 \\ If\ pro \geq rand \Rightarrow \text{ do nothing} \end{cases} \tag{53}$$

Pro is a parameter within an open interval (0,1).

Step 4 Handling boundary constraints

To deal with the violation of side constraints a harmony search-based handling approach specifies whether the violating component should be interchanged with a corresponding component of a random frame in VFM or be determined randomly in a search space.

$$\begin{cases} If\ HMCR < rand \Rightarrow \text{choose a random value from } \mathbb{S} \\ If\ HMCR \geq rand \Rightarrow \text{ choose a random value from RM,} \end{cases} \tag{54}$$

where HMCR is the harmony memory considering rate variable between 0 and 1.

Step 5 Termination criterion

The optimization process from steps 2 to 4 is performed successively until the preset maximum number of iterations. Eventually, the optimal frame is readily extracted from the VFM.

Step 6 Supplementary economizing techniques

The optimization process from steps 1 to 5 is repeated for a certain number of costlier deck slabs (n_r).

Step 7 Fine-tuning mechanism

The fine-tuning mechanism is executed.

The flowchart of the FT-VPS algorithm for cost optimization of steel–concrete composite castellated floor systems is illustrated in Fig. 5.

4.2 Formulation of ACS Algorithm with AS_{rank} Strategy

The ant colony system (ACS) is the best performing algorithm for combinatorial optimization problems with artificial ants (Siarry 2016). The formulation of ACS algorithm with AS_{rank} strategy for cost optimization of the steel buildings is delineated in the following literature. The first step in the application of ACS is to approximate an initial trail value. Typically, the initial value of *pheromone trail* on all the routes is set to a small positive constant as:

$$\tau_0 = \frac{1}{\sum C_{\min -frames}} \tag{55}$$

where $\sum C_{\min -frames}$ is the cost of the least-cost heuristic for the framing members of steel buildings. *Visibility* allows the ants to realize the cost of the routes. The invariant amount of visibility, v_{ij} associated with *j*th route of the *i*th path is:

$$v_{ij} = \frac{1}{C_{ij}} \tag{56}$$

Here, the cost of the routes connecting the paths is symbolized by C_{ij}. The ACS process follows the pseudo-code shown in Table 2.

Firstly, the initial nodes of the ants in the MTSP graph are determined randomly. The ACS process begins at time *t* when each ant chooses a route and traverses ahead to the corresponding destination node, where it is now at time $t+1$. The probability that the ant *k* decides *to* choose the *j*th route for traveling across the *i*th path at time t is obtained by combining visibility and local trail intensity in accordance with the following formula:

$$D_{ij}(t) = \frac{\tau_{ij}(t) \cdot v_{ij}^{\beta}}{\sum_{j=1}^{n_r^i} \tau_{ij}(t) \cdot v_{ij}^{\beta}}, \tag{57}$$

where n_r^i is the total number of routes for the i^{th} path. Thus, an iteration of the algorithm is defined as the m moves made by m ants in the time interval $(t, t+1)$. At the end of each iteration, after the decision is made and a route chosen, the intensity of the pheromone trail on the chosen route is lowered in order to promote exploration in the search. *Local update rule* prevents early stagnation of the search and premature convergence of the solution by the following relation:

$$\tau_{ij}(t) = \xi . \tau_{ij}(t), \tag{58}$$

where ξ is the adjustable parameter in the interval [0,1], representing the persistence of the pheromone trails. Each ant continues to choose routes for traveling across the paths until n_v iterations are completed and all paths have been visited.

Table 2 Pseudo code of the ACS algorithm for cost optimization of steel buildings

Repeat until	Fulfilment of stopping criteria (Round loop)
	Repeat until All the ants build up their trajectory (Trajectory loop)
	Ant decision mechanism
	Local pheromone trail update
	Terminate
	Ant memory mechanism
	Structural evaluation and fitness calculation
	Updating elitist ant checking convergence condition
	Global pheromone trail update
	Terminate

Each ant constructs a trajectory while having selected a solution for each of the design variables. The specific trajectories constructed by the ants are the solutions to the problem. In order to define how fit the solution are, the structural evaluation is to be performed. At the end of the trajectory loop (Table 2), firstly the ant memory mechanism is executed. Then the mathematical model of the spatial frames corresponding to the position of each one-off ant would be completed. Next, the constraints and the fitness of the frame designs would be assessed. Finally, the objective function of the one-off ant that is the total cost of the building, is reflected as a single numerical value. The design solutions created by the ants in a round are ranked according to their objective function values. The least-cost solution belongs to an *elitist ant* which will be updated in every iteration.

At this stage, the pheromone trail intensity upon each route of the developed trajectories is adjusted through a *global update process*. The global update process is performed by utilizing the AS_{rank} strategy that introduced a kind of contribution of the top-ranked ants for the trail update. The amount of pheromone to be added to the routes of the trajectories chosen by the top-ranked ants is calculated by:

$$\Delta\tau_{ij}^{top} = (n_{top} - n + 1)\frac{1}{C_n}, \tag{59}$$

where n_{top} is the number of the top ranked-ants; *n* is the rank of the ant (n = 1 to n_{top}); C_n is the fitness of the ant receiving rank *n*. Equation 59 is only used if the route connecting the node i to the node j is a part of the top-ranked trajectories, otherwise, it shall not be applied. The updated trail values at time $t+n$ are a function of the current pheromone values and the increase of trail level on edge (i, j) caused by the top-ranked ant. The expression of the global update scheme would be written as:

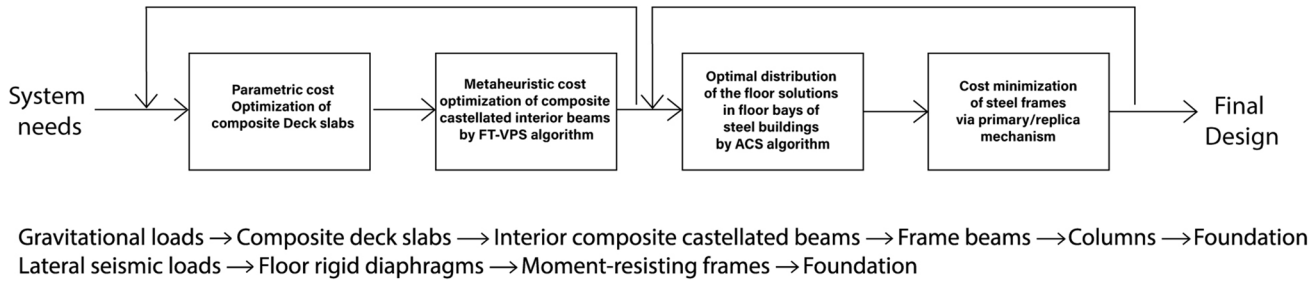

Fig. 1 Evolution model of the optimum design of steel buildings

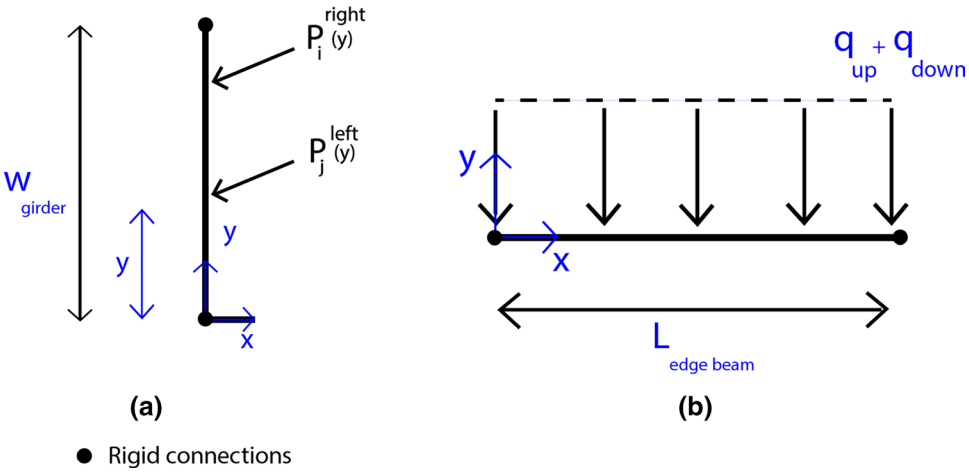

Fig. 2 General approach for decoupling the steel–concrete composite floor systems and spatial steel frames i = the numerator of the connecting interior beams in the right floor; j = the numerator of the connecting interior beams in the left floor q_{up} = uniform loads imposed by the floor above; q_{down} = uniform loads imposed by the floor below

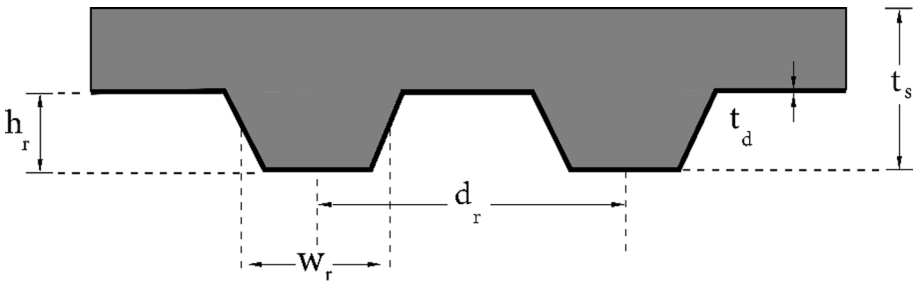

Fig. 3 Design variables of composite steel deck slabs

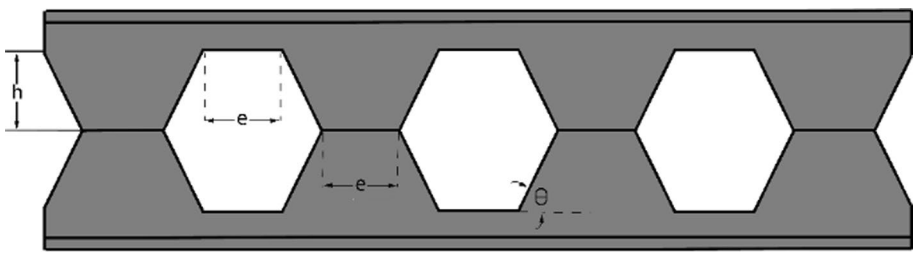

Fig. 4 Design variables of castellated beams

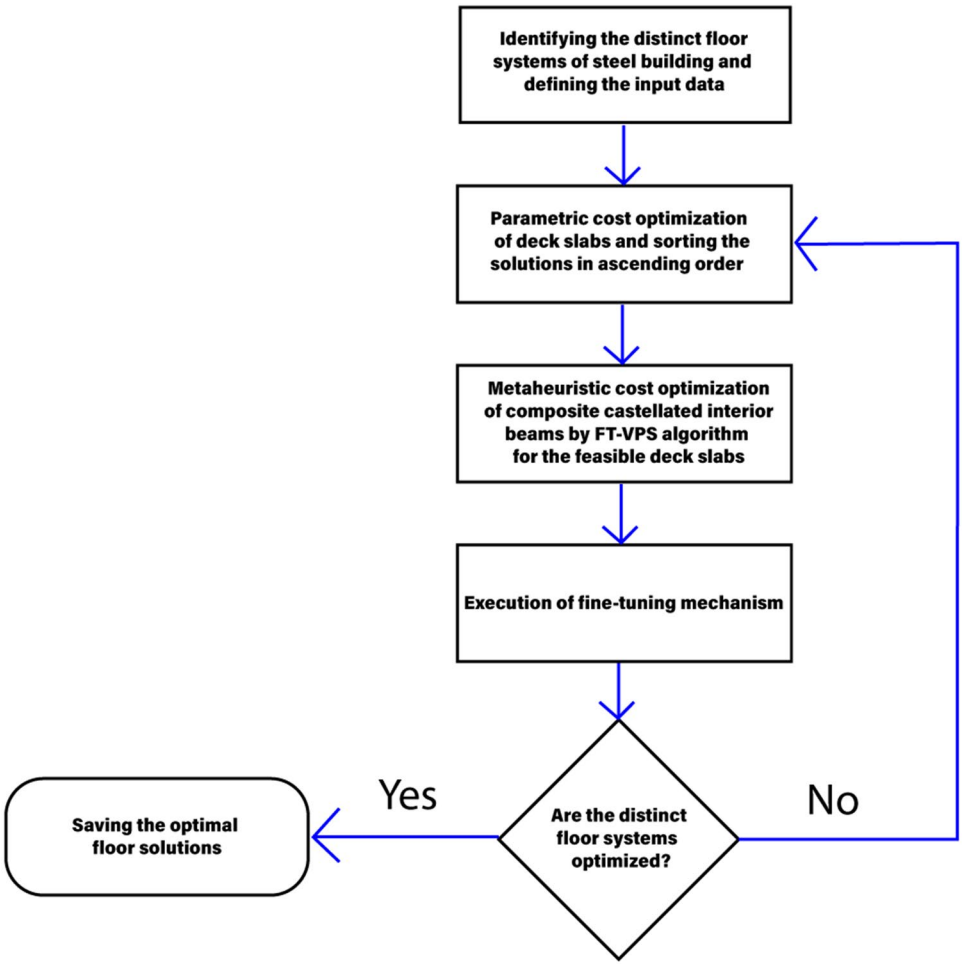

Fig. 5 Flowchart of the FT-VPS algorithm

$$\tau_{ij}(t+n) = (1-\rho)\,\tau_{ij}(t) + \rho\,\Delta\tau_{ij}^{top}, \tag{60}$$

where *(1- ρ)* represents the evaporation rate. At this point, the current round is complete, and a new round may be initiated and the entire process is repeated (Fig. 6). Eventually, most of the ants will select the same trajectory on every round, representing the convergence to the optimal solution. Here, two termination mechanisms are implemented concurrently. The first mechanism lets the algorithm's operation proceed until the predefined number of iterations (I_m). The second mechanism terminates the operation if the position of the elitist ant is not boosted up to the specified number of consecutive iteration (I_c). The flowchart of the ACS algorithm with AS_{rank} strategy for optimization of steel buildings is illustrated in Fig. 6.

5 Numerical Examples

5.1 General Statements

Two design examples are studied to validate the performance of the proposed optimization method. The MRSA procedure is used for earthquake simulation and seismic analysis. The design procedures of all the examples are performed in adherence with the 2016 version of AISC specifications (ANSI 2016).

The values of gravitational loadings and the magnitude of lateral earthquake loads for the first example is determined based on the Iranian National Building Code-Part 6 (INBC 6) (2020) and the Iranian code of practice for the seismic-resistant design of buildings (STD 2800-4) (Iranian

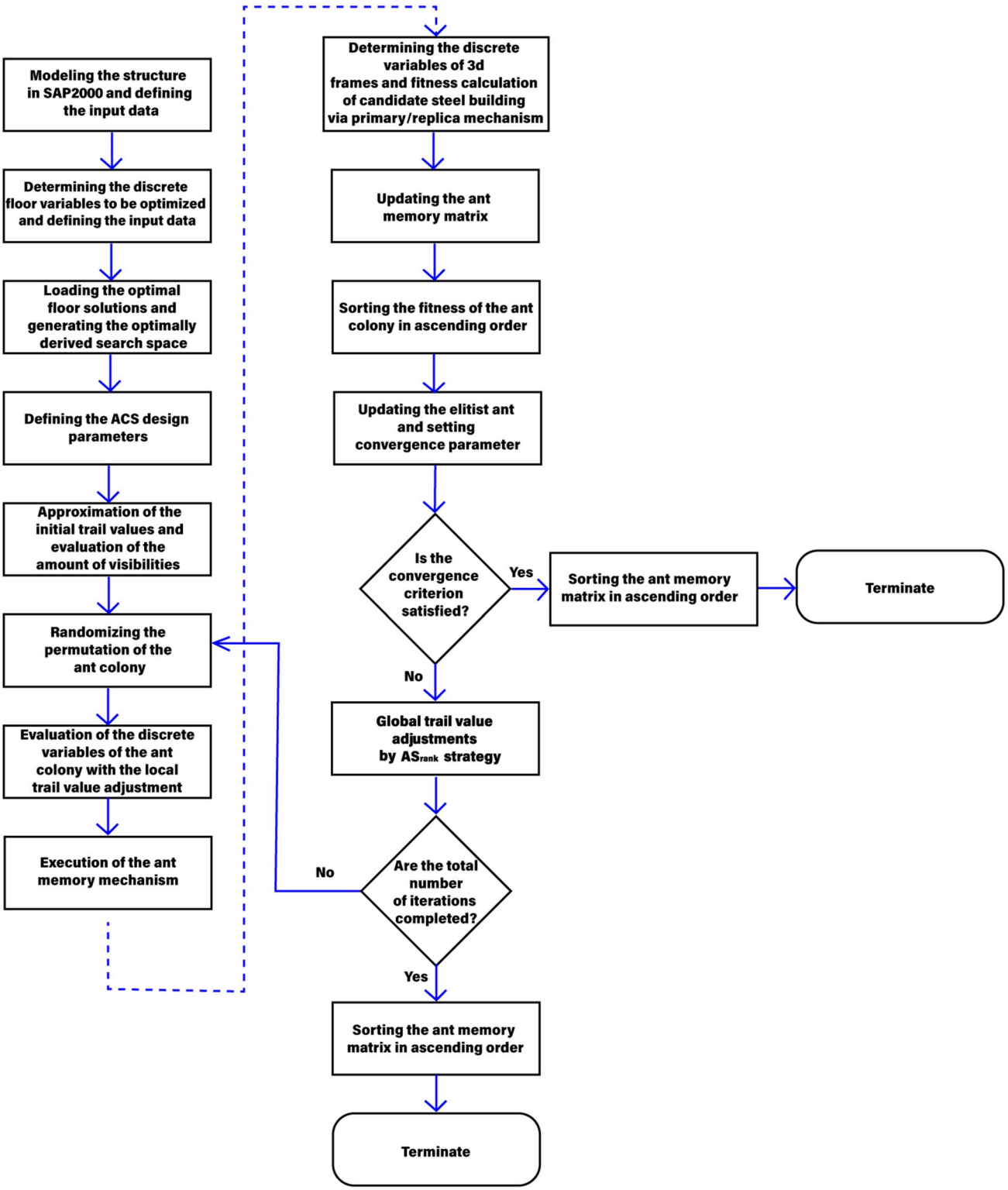

Fig. 6 Flow chart of the ACS algorithm with AS_{rank} strategy for optimization of asymmetrical-plan steel buildings

code of practice for seismic resistant design of Buildings-Standard 2014), respectively. The gravitational and seismic loadings of the second example are based on the ASCE 7–16 (ASCE 2016). Since the loading condition in all the stories is assumed to be identical, solely the geometry of the floor bays dictates the number of individual floor bays

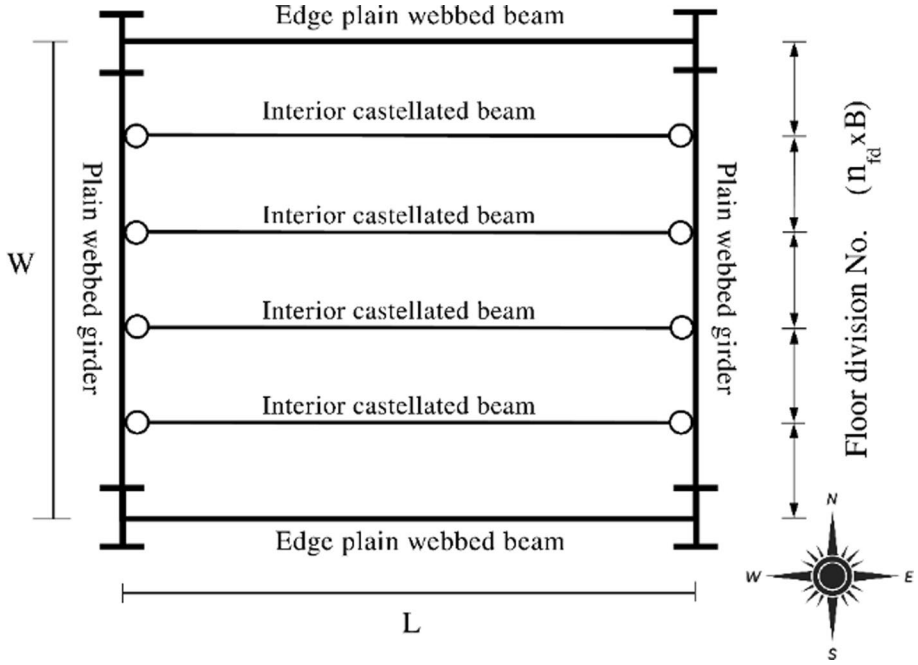

Fig. 7 Schematic of structural framing layout of the floor states

to optimize. The building occupancy of the examples is assumed to be an office.

Creep and shrinkage effects are considered in the deflection calculations of the floor members. A value of 4.2% of theoretical available damping is used for the examples. The type A welded stud of AWS D1.1/D1.1 M structural welding code (Code-Steel-AWS 2015) with $f_u = 420$ MPa and a diameter of 19 mm is utilized. Figure 7 schematically represents the structural framing layout of the floor states. The fixity conditions of beams and columns and also the column orientation whose strong axes are managed to act perpendicular to the orientation of girders are also sketched in the figure. The sensitivity analysis on the parameters of the VPS reveals that values 150, 0.05, 0.3, 0.3, 0.7 and 0.95 for the population size, c, ω_1, ω_2, *pro* and *HMCR* give rise to the most suitable performance (Kaveh and Ghazaan 2017).

The program is automated to interact with the SAP2000 for generating the mathematical model of the skeletal framing structure and conducting finite element analysis and LRFD based design procedures. Some of the main features taken into account in the mathematical model of the structure are expressed in the upcoming section. The structures are evaluated for stability in accordance with the direct analysis method. Second-order effects are accounted for by the exact method. The seismic part of the code and special seismic load combinations are also included.

The beams are modeled as laterally braced members and the fixity condition at the base of the frames are modeled as clamped. Each floor diaphragm is assumed to be rigid in its own plane, consequently, all the nodes at each floor level are constrained to the centroid of the diaphragms (Chopra 1995). Modal combinations of response spectrum load cases are performed by the complete quadratic combination (CQC).

The value of each force-related design parameter is multiplied by a $(I_e/R)g$. The values of redundancy factor (ρ) and the seismic importance factor (I_e) are considered as unity. The exterior beams of the buildings sustain the wall load applied by a ribbon window glazing system with brick spandrels 470 plf (700 kg/m). The floor height of the examples is considered as 13.5 ft ($\approx$ 4 m). The buildings in both of the examples are classified as *irregular* with geometrical reentrant corner irregularity.

We have triumphed in indicating that a value of $\beta = 1.5$ in the ACS algorithm helps enforce adequate feasibility while promoting an effective exploration within the search space. A value of $\xi = 0.1$ in the local pheromone reduction process provides a good balance between exploration and exploitation units. Computational efforts indicate that roughly 15 to 30 ants develop superlative solutions concerning the number of design variables. Regarding the AS_{rank} global update scheme, n_{top} is roughly equal to 10% of the number of ants and the value of $\rho = 0.7$ leads to acceptable results. The generic input data of the examples are tabulated in Table 3. In this study, twenty independent optimization runs are performed for locating a reasonably good final solution. The computing system used for this research is Intel (R) Core (TM) i5 CPU running at 2.4 GHz core speed with 8 Gb RAM.

Table 3 General input design parameters of optimization problems

Load types	Notations	Units	Values
Super imposed dead load	D_S	psf	51.2
Wall load	D_w	plf	470
Construction live load	L_c	psf	20
Actual live load	L_a	psf	11
Concrete density	γ_c	pcf	150
Steel density	γ_s	pcf	490
Elastic constant of steel	E_s	ksi	29,000
Concrete compressive strength	f'_c	ksi	5
Steel yield stress	F_y	ksi	50
Steel tensile strength	F_u	ksi	65
Diameter of shear stud	d_s	in	0.75
Tensile strength of shear stud	F_{us}	ksi	65
c/c of the ribs	d_r	mm	305
Available damping	ζ_c	%	4.2
Deflection limit for total load	δ_{at}	ft	L/240
Deflection limit for live load	δ_{al}	ft	L/360
Applying creep and shrinkage effect	δ_{per}	0 or 1	1
Cost factor of steel beams	k_s	\$/kips	341
Cost factor of concrete	k_c	\$/ft^3	4.8
Cost factor of steel deck	k_{sd}	\$/Ib	0.4
Cost factor of shear studs	k_{ss}	\$/Ib	0.45
Cost factor of welding	k_w	\$/ft	0.3
Cost factor of cutting	k_c	\$/ft	0.24
Cost factor of cambering	k_{ca}	\$/in	12.8
Cost factor of DS construction	$K_{\text{con-DS}}$	\$/ft^2	0.084
Story height	h_{story}	ft	13.5
Section pool of interior beams	W8 × 13	W44 × 335	ASTM W Sections
Section pool for framing members	W6 × 8.5	W44 × 335	ASTM W Sections
Deck slab section pool	–	–	Canam P-2432

5.2 Applied Loads and Load Combinations

The factored combination of super dead load, dead load due to the self-weight of DS, and reduced specified live load are the applied loads in the strength design of the composite DSs. The deflection criterion of the DSs is checked by the un-factored reduced specified live load.

The factored combination of super dead load, dead loads due to the self-weight of DS and CB, and reduced specified live load are the applied loads in the strength design of the interior composite CBs. The deflection criteria of the interior beams in the pre-composite stage are checked based on the un-factored loads, including dead loads due to self-weight of DS, and steel beam and construction live load, and in the post-composite stage are checked based on the super dead load and reduced specified live load.

After the optimization of floor systems, the resulting gravitational loads are distributed to the beam members of the moment-resisting frames. The uniform dead loads resulting from the exterior walls are applied to the perimeter beams of the frame systems. The lateral seismic loads are determined and distributed to the framing members based on the MRSA procedure.

The design strength of composite CBs must be equal to or greater than the effects of factored load in the following load combination:

$$LC^1_{CB} = 1.2\,D + 1.6\,L \tag{61}$$

Factored load combinations due to the gravitational and seismic effects for strength design of framing members prescribed by the ASCE 7 and INBC 6 are as follows:

$$LC^1_{frames} = 1.4D \tag{62}$$

$$LC^2_{frames} = 1.2D + 1.6L \tag{63}$$

$$LC^{3,4}_{\text{frames}} = 1.2D + 0.5L + 0.2S_{ds}D + \text{Spec}_{x,y} \tag{64}$$

$$LC^{5,6}_{frames} = 0.9D - 0.2S_{ds}D + Spec_{x,y}, \quad (65)$$

where D is the dead load; L is the minimum uniformly distributed live load, $Spec_{x,y}$ stand for the horizontal seismic load effects (E_h) in principal directions of the structure; The terms ($0.2S_{ds}D$) stand for vertical seismic load effects (E_v); S_{ds} is the design spectral response acceleration parameter at short periods.

Regarding visually unacceptable deformations and other short-term effects, the recommended service load combinations for the downward pull are:

$$LC^{1}_{def} = D + L \quad (66)$$

$$LC^{2}_{def} = L \quad (67)$$

5.3 Example 1

The 3-D view of a one-way asymmetrical-plan steel building with 2-story, 8-bay, and 46-member with composite castellated floor systems and moment resisting frames is illustrated in Fig. 8. The height of the building is 27 ft (≈ 8.2 m). The general input design parameters are summarized in Table 3. All steel members are ASTM A992 steel. The root beams of CBs are regarded as 233 W-shaped sections given in ASTM A6 starting from W8 × 13 to W44 × 335 sorted based on area properties. The set of composite deck slabs provided by P-2432 Canam profile are utilized. A combination of granite floor tiles, cement-mortar coating, and foam concrete covers the structural floors and, the hung ceiling provides enough space for housing the miscellaneous equipment (51.2 psf). The uniform construction live load of 20 psf (≈ 98 kg/m^2) is imposed on the floor systems. Additionally, the amount of 11 psf (≈ 54 kg/m^2) is considered for the weight estimate of the vibration control procedure. Inspection of the floor bays' geometries identifies three distinct states. The input design parameters specific to this example are tabulated in Table 4. The structural floor systems sustain the reduced level of prescribed distributed live load for office occupancy according to the provision of INBC 6. The minimal value of partition live load equal to 20.8 psf (≈ 102 kg/m^2) is taken into account.

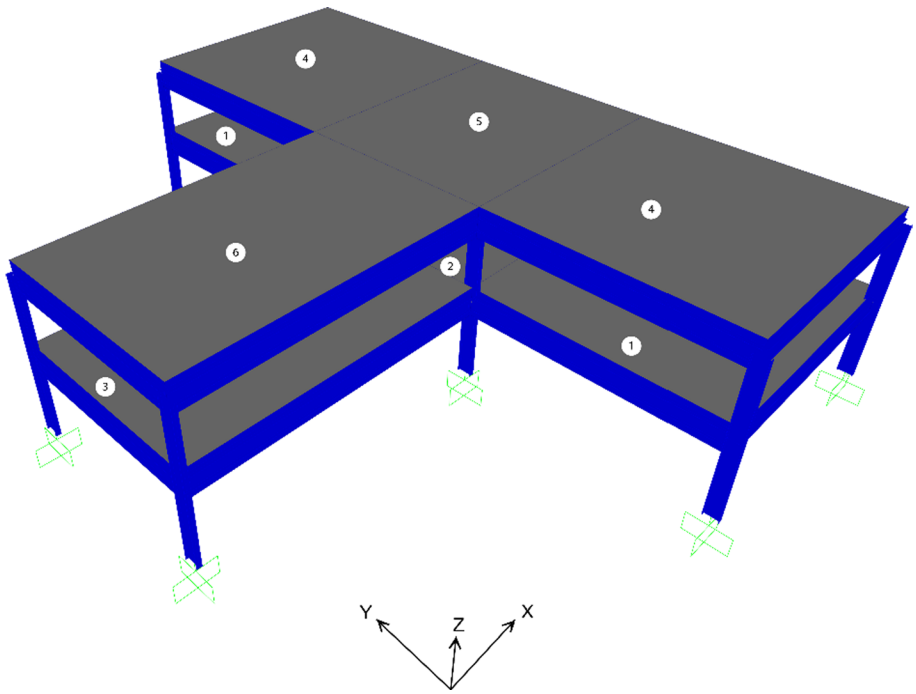

Fig. 8 3-D model of 2-story, 8-bay, 46-member building of Example 1

Table 4 Problem-specific input design parameters

Item	Notation	Unit	Floor state No		
			Floor 1	Floor 2	Floor 3
Floor span	L	ft (m)	40 (12.2)	40	50 (15.2)
Floor width	W	ft (m)	40	32 (9.75)	32
Reduced live load	L_{or}	psf (kg/m^2)	53.45 (260)	55.65 (270)	53.45

Table 5 Design variables and cost of the solutions of floor 1 (Search space of the floor systems which their state is identified as floor 1)

ID	RB	h	e	θ	N_{fd}	t_d	t_s	Cost
$\zeta_{1,1}$	W18×35	10	5	53.1	5	0.03	5	5585
$\zeta_{1,2}$	W21×44	11.8	5.9	53.1	4	0.036	5	5685
$\zeta_{1,3}$	W18×35	10	5	53.1	5	0.036	5	5810
$\zeta_{1,4}$	W21×44	11.8	5.9	53.1	4	0.036	5.5	6072
$\zeta_{1,nr}$	…	…	…	…	…	…	…	…
$\zeta_{1,15}$	W18×35	10	5	53.1	5	0.048	6.5	7470

The units of size and cost of floor components are inches and USD, respectively; ($n_r = 1$ to 15)
The costs of the solutions are rounded

Table 6 Design variables and cost of the solutions of floor 2

ID	RB	h	e	θ	N_{fd}	t_d	t_s	Cost
$\zeta_{2,1}$	W18×35	9.9	5	53.1	4	0.03	5	4370
$\zeta_{2,2}$	W18×35	9.9	5	53.2	4	0.036	5	4550
$\zeta_{2,3}$	W18×35	9.9	5	53.2	4	0.036	5.5	4860
$\zeta_{2,4}$	W21×44	11.8	5.9	53.2	3	0.048	5	4670
$\zeta_{2,nr}$	…	…	…	…	…	…	…	…
$\zeta_{2,15}$	W18×40	9.9	5.2	53.2	4	0.048	7.5	6445

Table 7 Design variables and cost of the solutions of floor 3

ID	RB	h	e	θ	N_{fd}	t_d	t_s	Cost
$\zeta_{3,1}$	W24×55	13.5	6.8	53.1	4	0.03	5	6485
$\zeta_{3,2}$	W24×55	13.5	6.8	53.1	4	0.036	5	6710
$\zeta_{3,3}$	W24×55	13.5	6.8	53.1	4	0.036	5.5	7100
$\zeta_{3,4}$	W24×62	13.5	6.7	53.1	3	0.048	5	6455
$\zeta_{3,nr}$	…	…	…	…	…	…	…	…
$\zeta_{3,15}$	W24×55	13.5	6.7	53.1	4	0.048	7.5	8820

The resulting design variables and cost of each of the floor state is illustrated in Tables 5, 6, 7, respectively (the tables are abridged by discarding 10 of the solutions). The required search space of the optimization process in the next phase is generated based on the results of this table. The notation $\zeta_{i,j}$ is utilized for the identification of each solution in which i stands for the number of floor states and j stands for the solution number. The convergence histories for the least-cost solution of each floor state at the onset of the fine-tuning mechanism are plotted in Fig. 9. The computing time of the floor optimization problems in the first phase equals 28 min and 30 s.

The grouping of the floor members considered in the second phase is illustrated in Fig. 8; hence, the number of floor design variables is equal to six. After defining the design variables, the resulting search space will be replicated accordingly for the complete generation of routes:

$$\begin{aligned} &\text{Floor}_{1j} = \eta_{1j};\ \text{Floor}_{2j} = \eta_{2j};\ \text{Floor}_{3j} = \eta_{3j} \\ &\text{Floor}_{4j} = \eta_{1j};\ \text{Floor}_{5j} = \eta_{2j};\text{Floor}_{6j} = \eta_{3j} \\ &\text{where } j = 1 \text{ to } 15 \end{aligned} \tag{68}$$

Frame members are selected within the auto-selection list of the SAP2000 consisting of 252 W-shaped sections starting from W6×8.5 to W44×335. The building is supposed to be located in Tehran. According to STD 2800, office buildings are categorized as a moderate risk category. It is assumed that the evaluation of the sub-soil determined the site class to be category two. The area is classified as the first category concerning relative seismic risk and has the ratio of design base acceleration to gravitational acceleration as $A = 0.35$. The design spectrum function of STD 2800 with a 5% of damping ratio is generated. Based on the risk category and relative seismic risk, it is not permitted to utilize OMF.

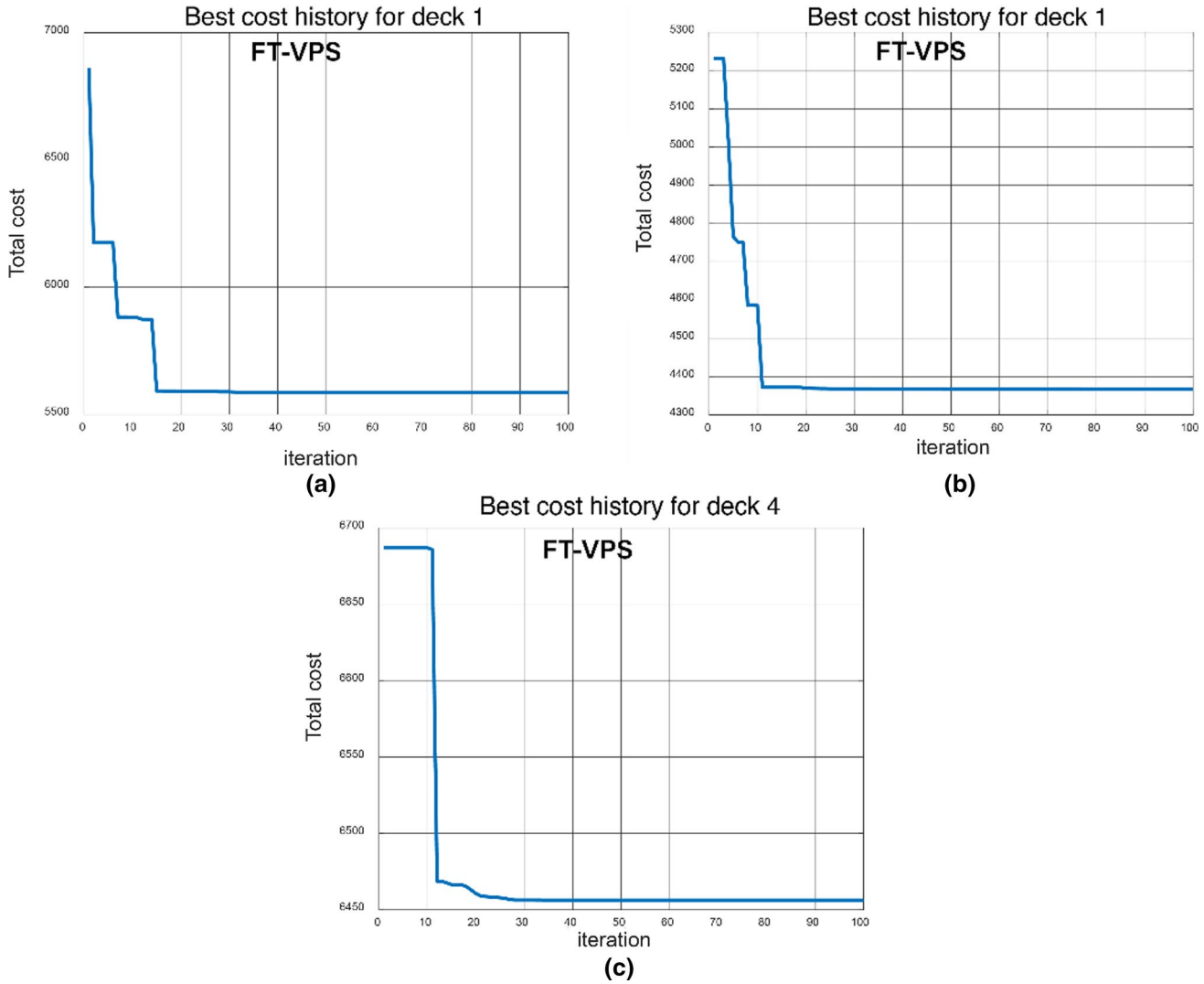

Fig. 9 Cost history graphs for the least-cost solutions of Example 1 by FT-VPS algorithm; **a** Floor 1, **b** Floor 2, and **c** Floor 3

Therefore, the IMF is utilized as the lateral load resisting system. The equivalent seismic design factors R_u, Ω_0, and C_d are 5, 3, and 4, respectively. The perimeter beams sustain the wall load of 470 plf (700 kg/m).

For transforming the structural configuration into the MTSP graph, two steps must be taken. In the first step, a costed cycle graph with the number of edges equal to the number of design variables of the floors (n_v) must be formed (the purple graph in Fig. 10). This initial simple graph provides adequate conditions for the adjacency of the nodes of the ultimate MTSP graph. Each pair of adjacent vertices that are incident by a single edge at this step represents an individual design variable for the floor systems. The cost of each edge $C_{i,1}(e)$ equates to the cost of the first design solution in the pertinent search space.

In the second step a *planar multiple-graph* should be formed. The number of edges that must be added to form new routes for each pair of incident vertices is equal to the number of solutions that could be assigned to each design variable, excluding the first solution ($n_r{}^i - 1$) which is 14 here. Similarly, the cost of each edge is equal to the cost of the solution that the edge symbolizes. The resultant graph is the MTSP graph associated with the optimum design of steel buildings depicted in Fig. 10. As it is also illustrated in the MTSP graph, the *optimum trajectory* found by the colony is (1,1,4,1,1,4). The best cost of the steel building for the optimal trajectory is \$79,733. Mathematically, the optimal set of floor design variables is to be written as $Floor_{1,1}$, $Floor_{2,1}$, $Floor_{3,4,}$ $Floor_{4,1}$, $Floor_{5,1,}$ $Floor_{6,4}$. The equivalent subordinate design variables pertinent to the framing members are illustrated schematically in Fig. 11a, b. The corresponding convergence history of optimal design of steel building is plotted in Fig. 12.

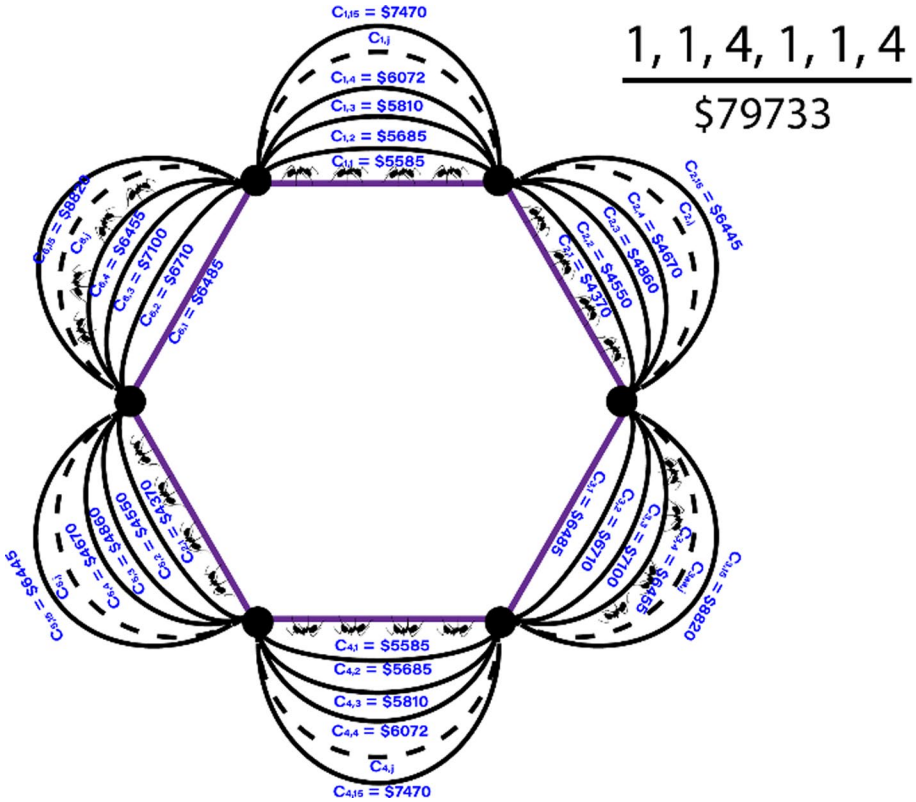

Fig. 10 MTSP graph with optimal cost and optimal trajectory of Example 1

The convergence graph in the second phase of the proposed optimization method (Fig. 12) is radically different from those in the first phase (Fig. 9). The search space of the composite castellated floor systems is derived from an optimization process which is naturally different from ordinary search space like commercially available sections of steel framing members. Additionally, exploring the discrete variables of the framing members is performed by the Auto-selection property of SAP2000, which is essentially different from that in the metaheuristics. In the initial iterations, the candidate solutions of steel framing members equivalent to the candidate distribution of the floor solutions explored by the provisional elitist ant, possess a low amount of infeasibilities. Nevertheless, the optimization method in the second phase could efficiently extract the flooring variables with their equivalent framing variables that reduce the steel building cost from $85,000 in the first iteration to $79,733 in the last iteration yielding a 6.2% reduction of the structural cost.

The number of ants and convergence parameter for this example is considered as 15 and 10, respectively. The total number of iterations are 36. The computing time of each ant is approximately 1 min and 20 s. The ant memory matrix contains the floor variables (i.e. floor distributions) and their equivalent building cost and floor cost of the one-off ants. The dimension of the ant memory matrix of the current example is 426×8. The ant memory matrix for the first 10 ants is shown below. The floor cost of the solution explored by the 4th ant in the ant memory matrix equals $33,000, which is higher than the cost of the 5th ant equals $32,920, however, the total cost of the 4th ant is lower. This result evinces that increasing the cost of floor solutions could reduce the cost of framing members by increasing the symmetry of the structure in a way that the resultant cost of the building is reduced. This pattern could be observed repeatedly in the ant memory matrix. The best cost, worst cost, mean cost, and the standard deviation resulting from twenty independent optimization runs are 79,732.6, 81,340.2, 80,802.8, and 348.1, USD, respectively.

$$\text{Ant Memory} = \begin{bmatrix} 79732.6 & 32820 & 1 & 1 & 4 & 1 & 1 & 4 \\ 79762.3 & 32850 & 1 & 1 & 1 & 1 & 1 & 4 \\ 79792 & 32880 & 1 & 1 & 1 & 1 & 1 & 1 \\ 79913.6 & 33000 & 1 & 2 & 4 & 1 & 1 & 4 \\ 79933.5 & 32920 & 2 & 1 & 4 & 1 & 1 & 4 \\ 79943.3 & 33030 & 1 & 1 & 1 & 1 & 2 & 4 \\ 79972.9 & 33060 & 1 & 1 & 1 & 1 & 2 & 1 \\ 79972.9 & 33060 & 1 & 2 & 1 & 1 & 1 & 1 \\ 79988.6 & 33075 & 1 & 1 & 2 & 1 & 1 & 4 \\ 79988.6 & 33075 & 1 & 1 & 4 & 1 & 1 & 2 \end{bmatrix} \quad (69)$$

5.4 Example 2

The optimum design example of a 3-story, 7-bay, 44-member two-way asymmetrical-plan steel building is envisaged.

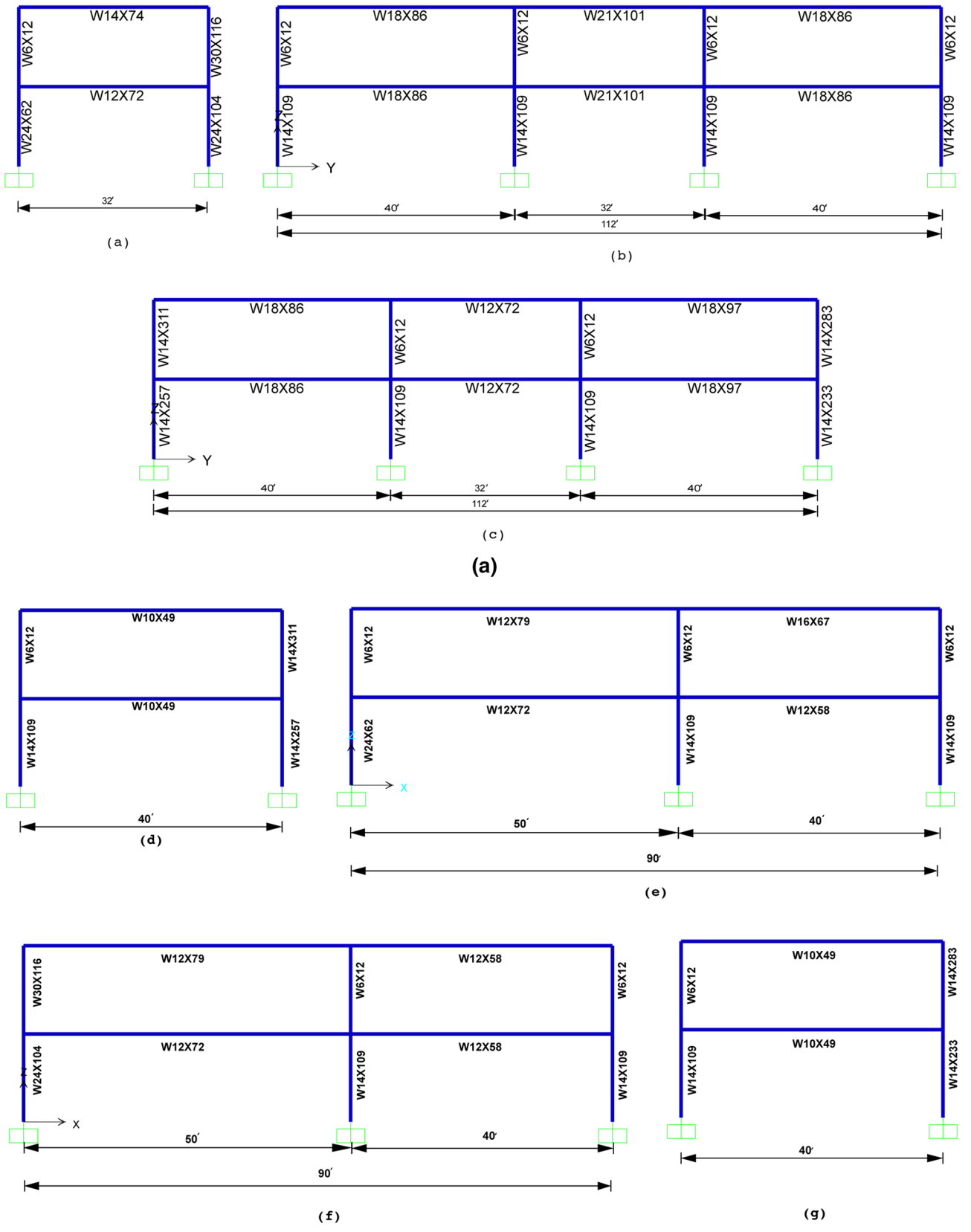

Fig. 11 **a** Side elevations of Example 1; (a) x = 0, (b) x = 50 ft, and (c) x = 90 ft. **b** Front elevations of Example 1; (d) y = 0, (e) y = 40 ft, (f) y = 72 ft, and (g) y = 112 ft

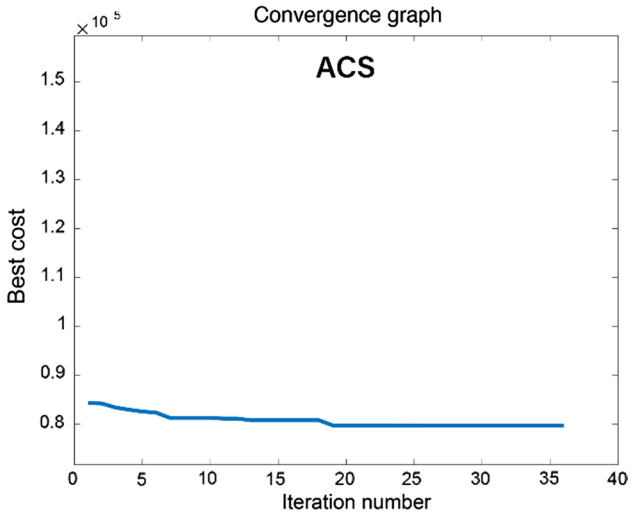

Fig. 12 Cost history plot for the optimal building of Example 1 by ACS algorithm

The centers of mass of all floor diaphragms do not lie on the same vertical axis. The 3-D model of the building is shown in Fig. 13. The height of the building is 40.5 ft.

The general input design parameters are summarized in Table 3. Inspection of the floor bays' geometries identifies four distinct states. The input design parameters specific to this example are tabulated in Table 8. The structural floor systems sustain the reduced level of live load for office occupancy according to the provision of ASCE 7–16. The minimal value of partition live load equal to 15 psf (≈ 73 kg/m^2) is taken into account.

The resulting design variables and cost of each of the floor state is illustrated in Tables 9, 10, 11, 12, respectively (the tables are abridged by discarding some of the intermediate solutions). The convergence histories for the least-cost solution of each floor state at the onset of the fine-tuning mechanism are plotted in Fig. 14. The computing time of the floor optimization problems in the first phase equals 36 min.

In the second phase, no grouping is considered for the floor members; therefore, the number of floor design variables is equal to seven. The equivalent routes are then generated in a similar manner as the previous example.

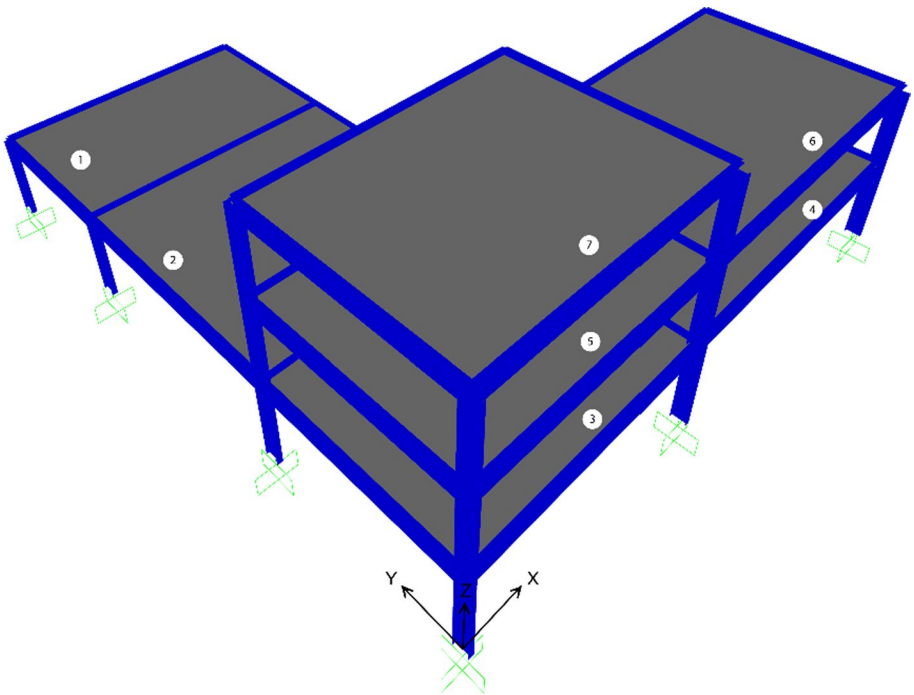

Fig. 13 3-D model of 3-story, 7-bay, 44-member building of Example 2

Table 8 Problem-specific input design parameters

Item	Notation	Unit	Floor state No			
			Floor 1	Floor 2	Floor 3	Floor 4
Floor span	L	ft (m)	40 (12.2)	40	40	50 (15.2)
Floor width	W	ft (m)	26 (7.9)	40	32 (9.7)	32
Reduced live load	L_{or}	psf (kg/m^2)	50.7 (247.5)	46.25 (225.8)	48.2 (235.3)	46.25

Table 9 Design variables and cost of the solution of floor 1 (Search space of the floor systems which their state is identified as floor 1)

ID	RB	h	e	θ	N_{fd}	t_d	t_s	Cost
$\zeta_{1,1}$	W18×40	10	5	53.1	3	0.036	5	3615
$\zeta_{1,2}$	W18×40	10	5	53.1	3	0.036	5.5	3870
$\zeta_{1,3}$	W18×40	10	5	53.1	3	0.048	5	3920
$\zeta_{1,4}$	W18×40	10	5	53.1	3	0.036	6	4030
$\zeta_{1,nr}$	…	…	…	…	…	…	…	…
$\zeta_{1,10}$	W18×40	10	5	53.1	3	0.048	8	5245

The units of size and cost of floor components are inches and USD, respectively; (n_r = 1–15)

Table 10 Design variables and cost of the solutions of floor 2

ID	RB	h	e	θ	N_{fd}	t_d	t_s	Cost
$\zeta_{2,1}$	W18×35	9.8	4.9	53.1	5	0.03	5	5585
$\zeta_{2,2}$	W18×40	9.9	5.1	53.4	4	0.036	5	5520
$\zeta_{2,3}$	W18×35	9.8	4.9	53.1	5	0.036	5	5810
$\zeta_{2,4}$	W18×40	9.9	5.3	53.7	4	0.036	5.5	5905
$\zeta_{2,nr}$	…	…	…	…	…	…	…	…
$\zeta_{2,15}$	W18×35	9.8	4.9	53.1	5	0.048	6.5	7295

Table 11 Design variables and cost of the solutions of floor 3

ID	RB	h	e	θ	N_{fd}	t_d	t_s	Cost
$\zeta_{2,1}$	W18×35	10	5	53.1	4	0.03	5	4365
$\zeta_{2,2}$	W18×35	10	5	53.1	4	0.036	5	4550
$\zeta_{2,3}$	W18×35	10	5	53.1	4	0.036	5.5	4860
$\zeta_{2,4}$	W21×44	11.8	5.9	53.1	3	0.048	5	4670
$\zeta_{2,nr}$	…	…	…	…	…	…	…	…
$\zeta_{2,15}$	W18×35	10	5	53.1	4	0.048	7.5	6365

Table 12 Design variables and cost of the solutions floor 4

ID	RB	h	e	θ	N_{fd}	t_d	t_s	Cost
$\zeta_{2,1}$	W24×55	13.5	6.8	53.1	4	0.03	5	6485
$\zeta_{2,2}$	W24×55	13.5	6.7	53.1	4	0.036	5	6710
$\zeta_{2,3}$	W24×55	13.5	6.7	53.1	4	0.036	5.5	7100
$\zeta_{2,4}$	W24×55	13.5	6.7	53.1	3	0.048	5	6205
$\zeta_{2,nr}$	…	…	…	…	…	…	…	…
$\zeta_{2,15}$	W24×55	13.5	6.8	53.1	4	0.048	7.5	8820

The building is supposed to be located in a Midwestern city with moderate seismic loads. The area has a short period $S_s = 0.121$ and a one-second period $S_1 = 0.06$ and long period transition $T_L = 12$ s. The site class is category D. For evaluation of the seismic loads in each mode of vibration, the design spectrum function of ASCE 7 with a 5% of damping ratio is generated. The seismic design category (SDC) of the building is defined as B and it is, therefore, legitimate to choose a moment-resisting frame not specifically detailed for seismic resistance. Thus, OMF is utilized as the seismic load resisting system and the corresponding seismic design factors R, Ω, and C_d are equated to values 3.5, 3, and 3, respectively. The MTSP graph is plotted similarly to the previous example. The optimal trajectory found by the colony in the equivalent MTSP graph is illustrated in Fig. 15. Mathematically the optimal floor distribution to the floor bays of the building is determined as: $\text{Floor}_{1,1}$, $\text{Floor}_{2,2}$, $\text{Floor}_{3,1}$, $\text{Floor}_{4,4}$, $\text{Floor}_{5,1}$, $\text{Floor}_{6,4}$, $\text{Floor}_{7,1}$. The corresponding optimal cost of the steel building is $80,889. The subordinate design variables of the framing members are represented schematically in Fig. 16a, b. The corresponding convergence history of optimal design of steel building is plotted in Fig. 17.

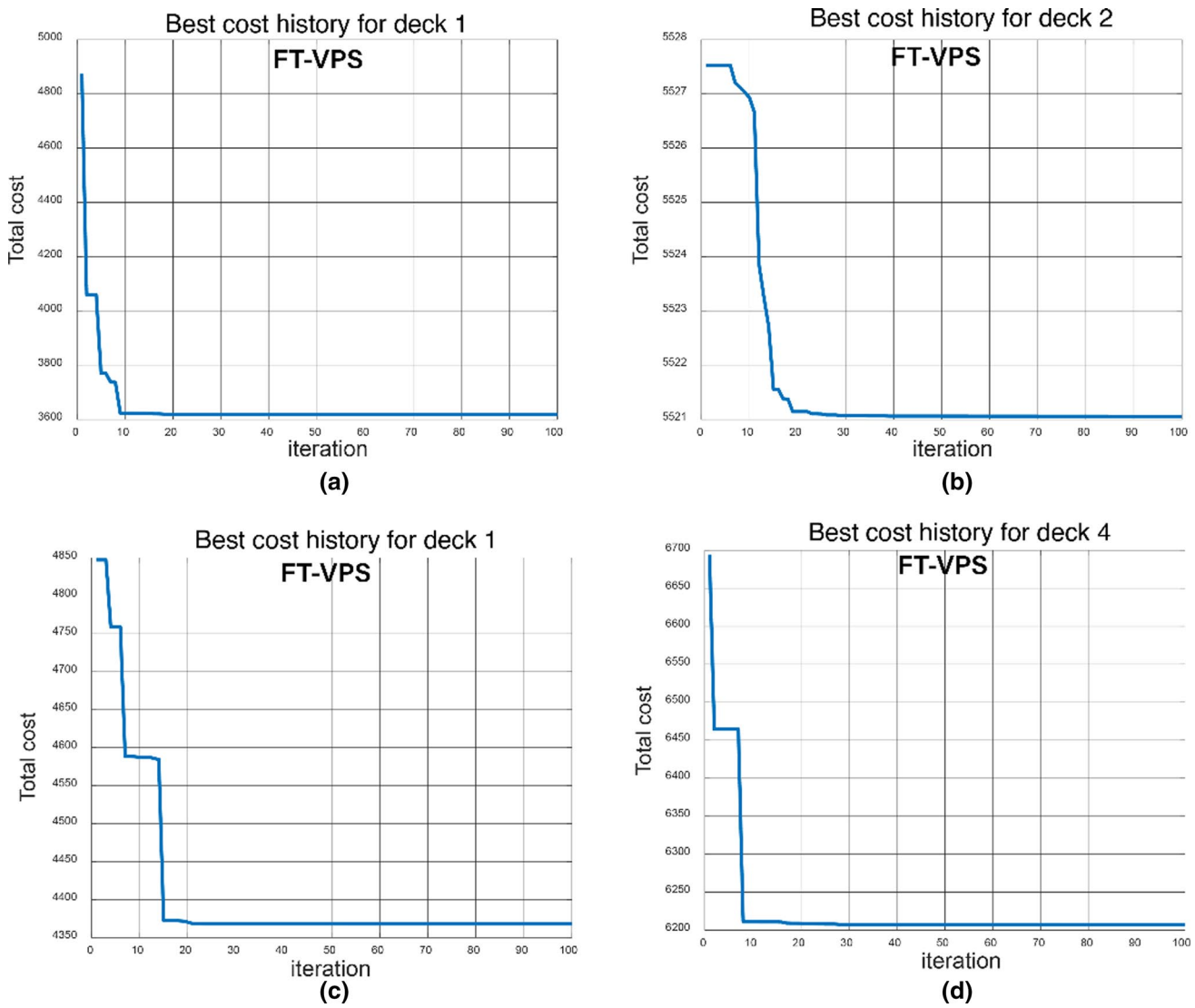

Fig. 14 Cost history graphs for the least-cost solutions of Example 2 by FT-VPS algorithm; **a** Floor 1, **b** Floor 2, **c** Floor 3, and **d** floor 4

The number of ants and convergence parameter for this example is considered as 20 and 10, respectively. The computing time of each ant was approximately 1 min and 35 s. The total number of iterations is equal to 43. The dimension of the ant memory matrix of the current example is 635×9. This matrix for the first 10 ants is shown below. The floor cost of the 7^{th} ant equals \$34,945 is higher than the cost of the 8^{th} floor equals \$34,895, but its total cost is lower. Increasing the cost of the floor systems may decrease the distance between centers of mass and rigidity, resulting in a reduction of the cost of framing members, reducing the total cost of the structure. This pattern could be observed in a number of intermediate solutions. The best cost, worst cost, mean cost, and the standard deviation resulting from twenty independent optimization runs are 80,889.3, 82,583.1, 81,646.1, and 409.7, USD, respectively.

$$\text{Ant Memory} = \begin{bmatrix} 80889.3 & 34640 & 1 & 2 & 1 & 4 & 1 & 4 & 1 \\ 81036.2 & 34705 & 1 & 1 & 1 & 4 & 1 & 4 & 1 \\ 81153.3 & 34825 & 1 & 2 & 1 & 4 & 1 & 4 & 2 \\ 81153.3 & 34825 & 1 & 2 & 2 & 4 & 1 & 4 & 1 \\ 81179.5 & 34930 & 1 & 3 & 1 & 4 & 1 & 4 & 1 \\ 81190.1 & 34945 & 1 & 2 & 1 & 4 & 1 & 4 & 4 \\ 81190.1 & 34945 & 1 & 2 & 1 & 4 & 4 & 4 & 1 \\ 81223.6 & 34895 & 2 & 2 & 1 & 4 & 1 & 4 & 1 \\ 81352.6 & 35105 & 1 & 6 & 1 & 4 & 1 & 4 & 1 \\ 81359 & 35025 & 1 & 4 & 1 & 4 & 1 & 4 & 1 \end{bmatrix} \quad (70)$$

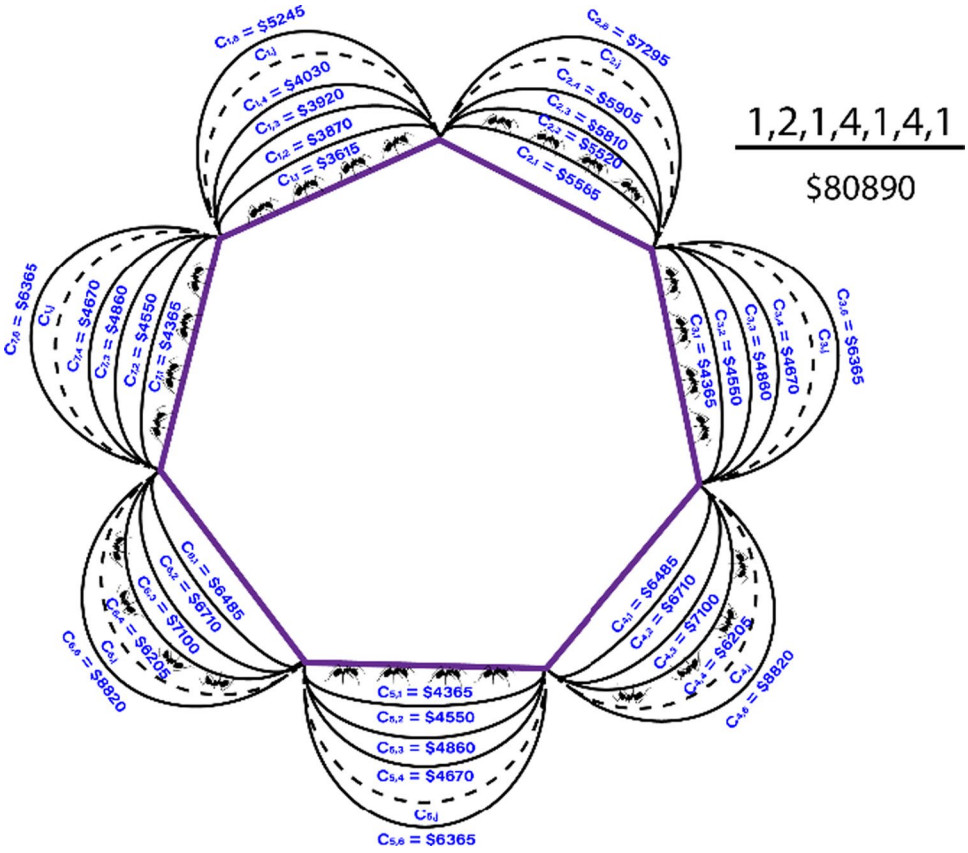

Fig. 15 MTSP graph with optimal cost and optimal trajectory of Example 2

6 Concluding Remarks and Limitations

The solution of the examples in the first phase demonstrated that the FT-VPS algorithm could successfully explore the optimal design variables governing the design of composite castellated floor systems. The supplementary cost reduction techniques for the floor systems have effectively averted cost escalation. The evidence deduced from the solutions implies that increasing the cost of deck slabs may well achieve a reduction in the total cost of the floor systems. As an essential requirement of the second phase, the FT-VPS could provide an optimal search space that contains various feasible solutions for distinct floor bays of asymmetrical-plan steel buildings. In the second phase, the ACS algorithm with AS_{rank} strategy could successfully explore the optimal distribution of the floor systems in the floor bays of the asymmetrical-plan steel buildings that its equivalent framing design led to the optimal resultant solution. In conclusion, the proposed cost optimization method optimally designs the main constituents of multistory asymmetrical-plan steel buildings considering their structural interaction.

The distribution of least-cost floor solutions in floor bays of asymmetrical-plan steel buildings was proved to be the optimal distribution. In some instances of the intermediate floor distributions, increasing the cost of floor systems could reduce the cost of framing members such that the total cost of the building is reduced. The ant memory matrix also provides a range of floor distributions with their equivalent framing design which could be utilized considering the constructional considerations. In addition, the unified two-phase function of the optimization method facilitates the vibration control of composite floor systems leads to the practicability of the design solutions. A new graph-based procedure for the formation of the MTSP network is applied in the examples.

We believe the present work has achieved the minimization of the consumption of material resources and maximizing structural efficiency. However, the proposed optimization method has limitations of its own and maybe enhanced by incorporating several capabilities. Possible future work needs to verify the lateral displacement constraints of the steel buildings, geometric constraints of the framing members, and also strong-column weak-beam criterion specific for SMFs. For comparative purposes, further studies should target the alternative optimization procedures for 3-D steel frames.

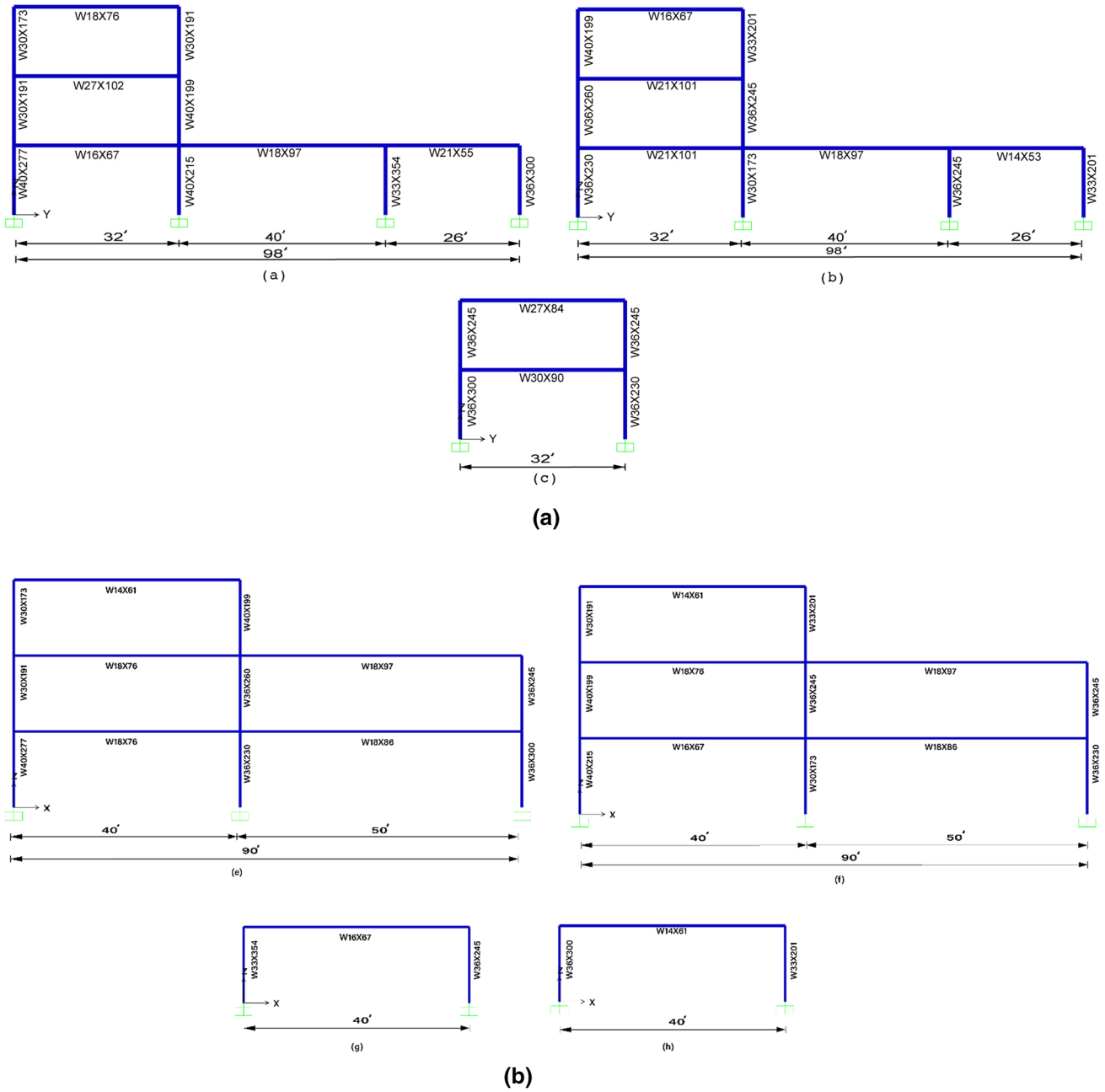

Fig. 16 **a** Side elevations of Example 2; (a) x = 0, (b) x = 40 ft and, (c) x = 90 ft. **b** Front elevations of Example 2; (a) y = 0, (b) y = 32 ft, (c) y = 72 ft and, (d) y = 98 ft

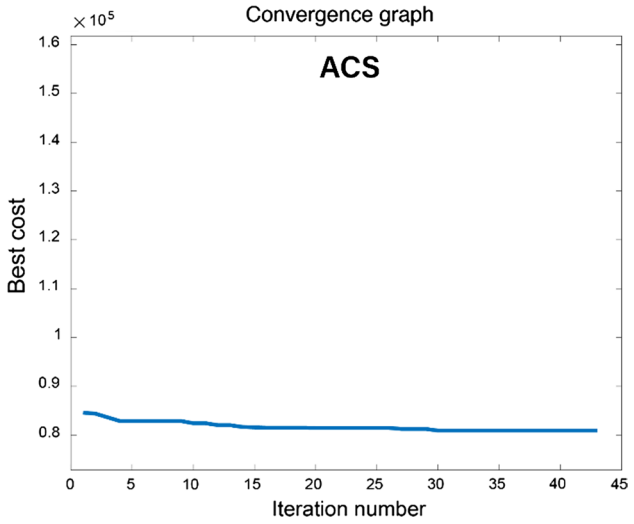

Fig. 17 Cost history plot for the optimal building of Example 2 by ACS algorithm

References

ANSI/AISC 360–16 (2016) Specification for structural steel buildings, American Institute of Steel Construction

Arora JS, Huang MW, Hsieh CC (1994) Methods for optimization of nonlinear problems with discrete variables: A review. Struct Optim 8(2):69–85

ASCE/SEI 7-16 (2016) Minimum design loads and associated criteria for buildings and other structures, American Society of Civil Engineers, New York

Aydoğdu İ, Saka MP (2012) Ant colony optimization of irregular steel frames including elemental warping effect. Adv Eng Softw 44(1):150–169

Azad SK (2019) Monitored convergence curve: a new framework for metaheuristic structural optimization algorithms. Struct Multidiscip Optim 60(2):481–499

Azad SK, Hasançebi O (2013) Upper bound strategy for metaheuristic based design optimization of steel frames. Adv Eng Software 57:19–32

Azad SK, Hasançebi O (2014) Computationally efficient optimum design of large scale steel frames. IUST 4(2):233–259

Benitez MA, Darwin D, Donahey RC (1998) Deflections of composite beams with web openings. J Struct Eng 124(10):1139–1147

Blodgett OW (1966) Design of welded structures. The James F. Lincoln Arc Welding Foundation, Cleveland

Bullnheimer B, Hartl R, Strauss C (1999) A new rank based version of the ant system - a computational study. CEJOR 7:25–38

Camp CV, Bichon BJ, Stovall SP (2005) Design of steel frames using ant colony optimization. J Struct Eng 131(3):369–379

Chopra AK (1995) Dynamics of structures, Theory and Applications to Earthquake Engineering. Pearson Education, Boston

CSI, "SAP2000 Integrated Software for Structural Analysis and Design,", Version 19.2.0, Computers and Structures Inc., Berkeley, California

Dorigo M, Di Caro G, Gambardella LM (1999) Ant algorithms for discrete optimization. Artif Life 5(2):137–172

Fares SS, Coulson J, Dinehart DW (2016) Castellated and cellular beam design, design guide 31. AISC, Chicago

Hasançebi O, Azad SK (2019) Discrete sizing of steel frames using adaptive dimensional search algorithm. Period Polytech Civ Eng 63(4):1062–1079

Hasançebi O et al (2010) Comparison of non-deterministic search techniques in the optimum design of real size steel frames. Comput Struct 88(17):1033–1048

Hasançebi O et al (2011) Optimum design of high-rise steel buildings using an evolution strategy integrated parallel algorithm. Comput Struct 89(21):2037–2051

Iranian code of practice for seismic resistant design of Buildings-Standard 2800 (2014) Road, Housing and Urban Development Research Center

Kaveh A, Fakoor A (2021) Cost optimization of steel-concrete composite floor systems with castellated steel beams. Period Polytech Civ Eng 65(2):353–375

Kaveh A, Ghafari MH (2016) Optimum design of steel floor system: effect of floor division number, deck thickness and castellated beams. Struct Eng Mech 59:933–950

Kaveh A, Ghafari MH (2018) Optimum design of castellated beams: effects of composite action and semi-rigid connections. Sci Iran 25(1):162–173

Kaveh A, Ghazaan MI (2017) A new meta-heuristic algorithm: vibrating particles system. Sci Iran 24(2):551–566

Kaveh A, Ghazaan M (2018) Optimum seismic design of 3D irregular steel frames using recently developed metaheuristic algorithms. J Comput Civ Eng 32(3):04018015

Kaveh A, Shokohi F (2015) Cost optimization of end-filled castellated beams using meta-heuristic algorithms. Int J Optim Civ Eng 5:333–354

Kaveh A, Shokohi F (2016) Optimum design of laterally supported castellated beams using natural forest regeneration algorithm. Iran J Sci Technol Trans Civ Eng 40(3):195–207

Kaveh A, Ghafari MH, Gholipour Y (2017) Optimal seismic design of 3D steel moment frames: different ductility types. Struct Multidiscip Optim 56(6):1353–1368

Kazemzadeh Azad S (2018) Seeding the initial population with feasible solutions in metaheuristic optimization of steel trusses. Eng Optim 50(1):89–105

Kazemzadeh Azad S (2021) Design optimization of real-size steel frames using monitored convergence curve. Struct Multidiscip Optim 63(1):267–288

MATLAB , Version 9.7 R2019b, The MathWorks, Inc., Natick, Massachusetts, United States

Murray TM (1991) Building floor vibrations. In: T.R. Higgins lectureship paper presented at the AISC National Steel Construction Conference. Washington

Naeim F (1991) Design practice to prevent floor vibrations. Structural Steel Educational Council, California

Poitras G, Cormier G, Nabolle A (2018) Novel optimization algorithm for composite steel deck floor systems: peloton dynamics optimization (PDO)

Safari D, Maheri MR, Maheri A (2021) Optimum design of steel frames using different variants of differential evolution algorithm. Iran J Sci Technol Trans Civ Eng 45(4):2091–2105

Siarry P (2016) Metaheuristics. Springer International Publishing, Switzerland

Steel Deck, Q. Canam Joists and steel Deck, 2006, Editor.

Structural Welding Code-Steel-AWS D1.1/D1.1M (2015) American Welding Society (AWS) D1 Committee on Structural Welding

The Iranian National Building Code-Part 6- Design loads for buildings (2020) Department of National Building Codes

Wilson RJ (1998) Introduction to graph theory, 4th edn. Longman Group Ltd, London